Supporting Information

Temperature Modulated Sustainable on/off Photosynthesis Switching of Microalgae towards Hydrogen Evolution

Shangsong Li, Zhijun Xu, Song Lin, Luxuan Li, Yan Huang, Xin Qiao, and Xin Huang*

MIIT Key Laboratory of Critical Materials Technology for New Energy Conversion and Storage, School of Chemistry and Chemical Engineering, Harbin Institute of Technology, Harbin, 150001 (China)
*E-mail: xinhuang@hit.edu.cn

Materials.
N-isopropylacrylamide (NIPAM, Energy, 98%) was purified by recrystallization in petroleum ether. Butyl acrylate (BA, Aladdin, 99%) was filtered twice in basic alumina. *Azo-bis*(isobutyronitrile) (AIBN, Energy, 98%) was purified by recrystallization in methanol. All other chemicals such as, 3-(3,4-dichlorophenyl)-1,1-dimethylurea (DCMU, Aladdin, 99.5%), Tetrahydrofuran (THF, Energy, 99.5%), Ether (Kermel, 99.5%), $[Ru(dpp)_3]Cl_2$ (MKbio), Fluorescein diacetate (FDA, Aladdin, 97%), Fluorescein O-methacrylate (Sigma-Aldrich, 95%) were used as received.

Additional characterization methods
Optical and fluorescence microscopy were performed on a Leica DMI8 manual inverted fluorescence microscope at ×20 and ×40 magnification. Scanning electron microscopy (SEM) images were obtained on a SU8000 instrument with the samples sputter-coated with 10 nm platinum. Zeta potentials were taken on Malvern Zetasizer Nano ZS90, and concentrations of PNIPAM-BA ranging from 0.0125 wt% to 0.1 wt% were chosen, which did not result in the formation of gel-state living materials. CLSM images and 3D CLSM videos were viewed with confocal laser scanning biological microscope (Leica TCS SP8, Germany). The pH measurements were made with a Seven Compact meter (Mettler Toledo, Sui). The concentration of hydrogen was measured with a hydrogen detector (Anpaer, China). The oxygen evolution was measured with a dissolved oxygen meter-F4 (Mettler Toledo, Sui). The lower critical aggregation temperature (LCAT) of PNIPAM-BA was determined by measuring turbidity of a 0.1 wt% PNIPAM-BA suspension in BG-11 at a wavelength of 650 nm using a PerkinElmer UV-Vis-NIR spectrometer (Lambda 750S, USA). Synthesis of PNIPAM-BA was confirmed by ^{1}H NMR (BRUKER, SUI). The molecular weight of PNIPAM-BA was determined by using Gel permeation chromatography (GPC). The thermogravimetric curve was measured by a differential thermal-thermogravimetric analyzer (Waters, USA) at a heating rate of 10 °C/min under N_2 purging at 50 mL/min in alumina crucibles, and the DTG curve was obtained by derivation of TG. The mechanical properties of GSLM and SSLM were characterized using rheometers with plate geometries of 20 mm and 60 mm, respectively. (Malvern, UK). Isothermal titration calorimetry experiments were performed on a micro 200 ITC isothermal titration calorimeter (Malvern, UK). F_V/F_M was measured by chlorophyll fluorometer (Yaxin-1161G, China). Cryo-SEM images were acquired on a FEI Quanta 450 Environmental Scanning Electron Microscope (FEI, USA) equipped with a PP3000T Cryopreparation Transport System (Quorum, UK). ImageJ software was used to count the number of cells and the percentage of fluorescent area.

Synthesis and characterization of poly(NIPAM-co-BA)
Copolymer of NIPAM and BA (PNIPAM-BA) was synthesized using free radical polymerization. A solution of NIPAM (4.75 g), BA (0.25 g), and AIBN (0.021 g) was dissolved in 60 mL of dry tetrahydrofuran (THF). The magnetically stirred solution was degassed for 40 min, heated to 50 °C for 24 hours under positive argon pressure. After polymerization, ether was added to precipitate the copolymer. The precipitate was filtered off, washed with ether, and dried under vacuum to yield dry 3.85 g of copolymer product. We prepared 5 wt% solution of PNIPAM-BA in $CDCl_3$ and used ^{1}H NMR to confirm the synthesis of target product. Green fluorescently labeled PNIPAM-BA was obtained by AIBN-initiated radical polymerization of NIPAM, BA, and Fluorescein O-methacrylate (molar ratio: 210:10:1).
The suitable growth temperature of *Chlorella* is between 20 – 30 ^{o}C. The lower critical solution temperature (LCST) of PNIPAM alone is 32 ^{o}C, and copolymerization of NIPAM with hydrophobic monomers can yield copolymers with lower LCST. Therefore, we carefully controlled the feeding ratio of hydrophobic monomer BA and NIPAM monomer to obtain

PNIPAM-co-BA copolymer with LCST of 25 ºC. At 20 ºC (< LCST), the *Chlorella* in SSLM can realize the physiological activities consistent with the natural state, such as photosynthesis, oxygen production and proliferation. At 30 ºC (> LCST), the *Chlorella* in GSLM display properties of photosynthetic hydrogen production due to shading effect.

Microalgae cell cultures

Culture *Chlorella* cells with TAP medium in a lighted incubator (temperature: 25 °C; light intensity: 50 $\mu E \cdot m^{-2} \cdot s^{-1}$; 12 h light and 12 h dark). The culture flasks were artificially shook three times per day. *Chlorella* cells were harvested in late logarithmic growth phase for experiments. The concentration of *Chlorella* cells was determined by the absorbance at 680 nm (OD_{680}). The components of TAP medium were as follows: NH_4Cl (0.375 g/L), $MgSO_4 \cdot 7H_2O$ (0.1 g/L), $CaCl_2 \cdot 7H_2O$ (0.05 g/L), K_2HPO_4 (1.08 g/L), KH_2PO_4 (0.54 g/L), Tris (2.42 g/L), Hutner's trace elements (1 mL/L), and glacial acetic acid (1 mL/L). The medium pH was adjusted to 7.0, and it was used after high temperature sterilization.

Preparation of SSLM and GSLM

The SSLM consisted of 7.55×10^7 cells/mL of *Chlorella* and 5 wt% of PNIPAM-BA at 20 °C. 2 mL of SSLM was transferred to a sealed tube and placed in a 30 °C water bath for 1 hour to obtain GSLM. Added 2 mL of medium to the sealed tube to provide the necessary elements for the *Chlorella*. Transferred the sealed tube containing the GSLM to 4 °C. The GSLM slowly liquefied and the SSLM would be recovered. For cell viability and chlorophyll concentration experiments, liquefaction of GSLM to SSLM was required. The *Chlorella* cells were then collected by centrifugation, washed 3 times with deionized water, and finally used for the above-mentioned tests.

Chlorophyll fluorescence kinetics measurements

The photosynthetic activity parameter F_V/F_M of *Chlorella* was assessed by fast chlorophyll fluorescence kinetic curves using a Yaxin-1161G chlorophyll fluorometer. For natural *Chlorella*, 2 mL of *Chlorella* suspension was added to the sample dish and placed in the dark for 30 minutes, so that the PSII reaction center was completely opened and the electron transport chain was completely oxidized. Then, put the sample dish into the liquid phase detector of the chlorophyll fluorometer for measurement. For *Chlorella* in GSLM, to prevent the influence of PNIPAM-BA on chlorophyll fluorescence, GSLM was transformed into SSLM to release encapsulated *Chlorella*, then the *Chlorella* were centrifuged to redisperse into BG-11 medium, and incubated for 2 hours in light and 30 minutes in dark for assay.

Photosynthetic oxygen/hydrogen production

For individual *Chlorella* cells, 2 mL of *Chlorella* suspension was transferred to a serum bottle (5 mL). Serum bottle was then placed in a lighted incubator at a light intensity of 50 $\mu E \cdot m^{-2} \cdot s^{-1}$. For GSLM, 2 mL of SSLM was transferred to serum bottle (5 mL), which was then placed in a 30 °C water bath to facilitate the conversion of SSLM to GSLM. After the GSLM had formed, transferred the serum bottle to a 30 °C lighted incubator with a light intensity of 50 $\mu E \cdot m^{-2} \cdot s^{-1}$. For the gel-sol switching of the material, the GSLM was formed at 30 °C and placed under a light intensity of 50 $\mu E \cdot m^{-2} \cdot s^{-1}$ for the specified time. The GSLM was transferred to 4 °C for 2 hours to obtain SSLM. The SSLM was then placed under a light intensity of 50 $\mu E \cdot m^{-2} \cdot s^{-1}$ at 20 °C for a specified time, and performed a specified number of cycles. Hydrogen detector (AP-B-H2-F; Max Range, 1000 or 5000 ppm; Resolution, 1 ppm) and dissolved oxygen meter (F4; Max Range, 45 mg/L; Resolution, 0.01 mg/L) were used to measure the concentration of hydrogen and oxygen in serum bottles, respectively. Algae were continuously illuminated under 50 $\mu E \cdot m^{-2} \cdot s^{-1}$ light intensity during the determination of hydrogen production. The serum bottle equipped with a T-shaped three-way joint was

connected to the hydrogen detector with a rubber catheter, and then the circulating gas pump of the hydrogen detector was turned on, and the hydrogen concentration data was recorded when the data was stable.
BG-11 and TAP medium were selected as the medium for hydrogen production. The components of BG-11 medium were as follows: $NaNO_3$ (1.5 g/L), Na_2CO_3 (0.02 g/L), K_2HPO_4 (0.04 g/L), $MgSO_4 \cdot 7H_2O$ (0.075 g/L), $CaCl_2 \cdot 2H_2O$ (0.036 g/L), citric acid (6 mg/L), ferric ammonium citrate (6 mg/L), EDTA Na_2 (1 mg/L), and trace metal solution (1 mL/L). The trace metal solution consisted of H_3BO_3 (2.86 g/L), $MnCl_2 \cdot 4H_2O$ (1.86 g/L), $ZnSO_4 \cdot 7H_2O$ (0.22 g/L), $Na_2MoO_4 \cdot 2H_2O$ (0.39 g/L), $CuSO_4 \cdot 5H_2O$ (0.08 g/L), and $Co(NO_3)_2 \cdot 6H_2O$ (0.05 g/L).The medium pH was adjusted to 7.0, and it was used after high temperature sterilization.

Measurement of ATP content
For SSLM, *Chlorella* were collected by centrifugation at 6000 rpm for 5 min. For GSLM, *Chlorella* were collected by centrifugation after liquefaction at 4 °C. The collected *Chlorella* were washed three times with PBS solution (pH = 7.4), and then intracellular ATP was extracted by repeated alternating freezing and thawing cycles. The samples were centrifuged at 6000 rpm for 5 min and the supernatant was collected. The concentration of ATP was determined spectrophotometrically using an ATP Elisa kit (Institute of Detection Technology, Shanghai, China).

Measurement of $NADP^+$/NADPH content
For SSLM, *Chlorella* were collected by centrifugation at 6000 rpm for 5 min. For GSLM, *Chlorella* were collected by centrifugation after liquefaction at 4 °C. The collected *Chlorella* were washed three times with PBS solution (pH = 7.4), and resuspended in 1 mL of cell lysis buffer, followed by sonication for 30 min in ice bath. The samples were centrifuged at 6000 rpm for 5 min and the supernatant was collected. The concentration of $NADP^+$/NADPH was determined spectrophotometrically using the $NADP^+$/NADPH Elisa Kit (Institute of Detection Technology, Shanghai, China).

Correlation standard curve of *Chlorella* concentration and OD_{680}
Chlorella suspensions with different OD_{680} were prepared. The number of *Chlorella* per unit volume was measured with a hemocytometer, and then the OD_{680} was correlated with the *Chlorella* concentration (Cc) by a standard curve. The standard curve equation was as follows:
$Cc\ (cells/mL) = 1.03 \times 10^7\ OD_{680} - 5.60 \times 10^5,\ R^2 = 0.96$ (1)

Cell viability tests
Dissolved FDA in acetone (5 mg/mL) and transferred 5 μL of the solution to a centrifuge tube containing 1 mL of *Chlorella*. After incubation for 30 min at room temperature, *Chlorella* were washed 3 times with deionized water and imaged using a fluorescence microscope. Green fluorescence was from viable *Chlorella* and red fluorescence was from intracellular chlorophyll. The ImageJ software was used to count the number of *Chlorella* emitting red (Nr) and green fluorescence (Ng), respectively. The *Chlorella* survival ratio was calculated by the following equation:
Chlorella survival ratio (%) = $Ng/Nr \times 100\%$ (2)

Determination of chlorophyll content
For native *Chlorella*, *Chlorella* were collected by centrifugation at 6000 rpm for 5 min. For GSLM, *Chlorella* were collected by centrifugation after liquefaction at 4 °C. The collected *Chlorella* were washed 3 times with deionized water. After centrifugation, the supernatant was removed and 100 μL of ethanol was added. Placed the homogenized mixture at 4 °C for

at least 12 h. The mixture was then centrifuged and the chlorophyll concentration in the supernatant was determined by spectrometry from absorbance values at 665 nm (A_{665}) and 649 nm (A_{649}). Calculated the total concentration of chlorophyll (C, μg/mL) using the following equation:

$$C = 6.1 \times A_{665} + 20.04 \times A_{649} \quad (3)$$

Encapsulation efficiency of GSLM for *Chlorella*.

The initial concentration of *Chlorella* in the SSLM was determined by OD_{680}. After forming GSLM, the upper liquid in the sealed tube was aspirated and the *Chlorella* were collected by centrifugation. The *Chlorella* were redispersed in water and the OD_{680} was determined to obtain the residual *Chlorella* concentration. The encapsulation rate of *Chlorella* by GSLM and the number of *Chlorella* encapsulated in GSLM were obtained by initial concentration and residual concentration.

Rheology of Living Material

The mechanical properties of GSLM and SSLM were characterized using rheometers with plate geometries of 20 mm and 60 mm, respectively. For all experiments, an integrated Peltier plate was used to control the temperature and a solvent trap was utilized to minimize solvent evaporation. The GSLM was investigated with strain-amplitude sweeps at 30 °C with the amplitude varying from 0.01 to 1% strain and a frequency of 1 Hz. After the critical strain was found for GSLM, oscillation tests were performed to measure the loss (G″) and storage (G′) moduli at 30 °C. Strain was fixed at 0.01% (below the critical strain), and moduli were measured as a response to logarithmic angular frequency ramp from 0.1 to 10 Hz. For the SSLM strain sweep experiments were performed with the amplitude varying from 0.1 to 100% strain and a frequency of 1 Hz. Similarly, frequency sweep experiments were performed with an amplitude of 0.1 to 10 Hz and a strain of 1%. The shear viscosity of SSLM was investigated as a function of shear rate (10^{-4} to 10^{1} s^{-1}) using a 60 mm flat plate at 20 °C.Time dependent changes in G' and G" on living material were performed using a fixed angular frequency of 1 Hz and 0.01% strain on a 20 mm flat plate.

Isotherm titration microcalorimetry

ITC experiments were performed using MicroCal ITC200 (Malvern, UK). The reference and sample cells of the calorimeter were filled with high-purity water and PNIPAM-BA solution (0.0125 wt%, 200 μL), respectively. The titrant syringe was filled with *Chlorella* suspension (2.05×10^{8} cells/mL,40 μL). For each experiment, performed 20 injections of 2 μL of the *Chlorella* suspension (initial injections of 0.4 μL, each lasting 4 s) at 150 s intervals to allow sufficient time for the system to return to the experimental baseline. Corresponding control experiments to determine the heat of dilution of PNIPAM-BA and *Chlorella* suspensions were performed by injecting the same volume of buffer solution into the PNIPAM-BA solution and *Chlorella* suspension into the buffer solution, respectively. The reference power and stirring speed were kept at 5 μcal·s^{-1} and 600 rpm throughout the experiment. The resulting corrected injection heat was plotted as a function of *Chlorella*/PNIPAM-BA molar ratio and fitted using Origin 7.0 software.

Hydrogen suppression by DCMU

The stock solutions of DCMU were prepared by dissolving 0.05 g of DCMU in 20 mL of acetone. For the suppression of hydrogen production on the *Chlorella*, 40 μL of DCMU solutions were added into the serum bottle with a final concentration of 100 μM.

In vivo hydrogenase activity

For the in vivo measurement of hydrogenase activity, *Chlorella* alone and GSLM were immediately sparged with argon gas for 2 min to eliminate the inhibitory effect of O_2 on hydrogenase. Next, the samples were placed in a 30 °C water bath for 1 h under continuous shaking (150 rpm) and exposed to a light intensity of 50 $E \cdot m^{-2} \cdot s^{-1}$. The in vivo hydrogenase activity was then calculated on the basis of the total chlorophyll content in the serum bottle.

SEM characterization of living material

The SSLM was placed in a 30 °C water bath for 1 minute and 2 hours, respectively, removed and snap-frozen in liquid nitrogen. Subsequently, water was removed from the frozen living material by freeze-drying for 2 days. The dried samples were freeze-fractured using liquid nitrogen and sputtered with gold using a SC7640 high-resolution sputter coater (Quorum Technologies) at 2.0 kV and 20 mA for 15 s. Subsequently, the gold-plated samples were imaged using SEM.

Cryo-SEM characterization of living material

Sample was frozen and fixed by liquid nitrogen mud method, and then transferred to a vacuum sputtering apparatus under freezing conditions for fracture, exposing the fresh fracture surface of the sample. The fractured surface of the sample was sublimated at -90 °C for 10 minutes, and sputtered with gold at a current of 10 mA for 60 s, and then sent to the sample chamber of a scanning electron microscope for observation. The temperature of the cold stage was -140 °C, and the accelerating voltage was 5 kv.

Oxygen indicator to detect the anaerobic state of *Chlorella*

The anaerobic state of natural *Chlorella* and *Chlorella* in living materials was investigated by confocal fluorescence imaging using the oxygen indicator $[(Ru(dpp)_3)]Cl_2$. The fluorescence of oxygen indicator was quenched under aerobic conditions and excited under anaerobic conditions. For the native *Chlorella* anaerobic assay, *Chlorella* were incubated with 5×10^{-6} M $[Ru(dpp)_3]Cl_2$ for 12 h. The fluorescence signal of $[Ru(dpp)_3]Cl_2$ (Ex 488 nm, Em 610 nm) in the cells was then observed and photographed under CLSM. For the *Chlorella* anaerobic assay in GSLM, *Chlorella*, PNIPAM-BA and 5×10^{-6} M $[Ru(dpp)_3]Cl_2$ were incubated together at 30 °C for 12 h. The formed GSLM was then sliced, and the fluorescence signal of $[Ru(dpp)_3]Cl_2$ (Ex 488 nm, Em 610 nm) in the GSLM was observed and photographed under CLSM.

Correlation standard curve of *Chlorella* dry weight and OD_{680}

The *Chlorella* suspension was washed three times with deionized water, and then *Chlorella* suspensions with different OD_{680} were prepared. The *Chlorella* suspensions were lyophilized for 48 h, and the dry cell weight (DCW) of the *Chlorella* was recorded. The OD_{680} was correlated to the DCW of *Chlorella* by a standard curve. The standard curve equation was as follows:

$$DCW\ (g/L) = 0.2899 \times OD_{680} - 0.0022,\ R^2 = 0.99 \quad (4)$$

Measurement of carbohydrate content

For SSLM, *Chlorella* were collected by centrifugation at 6000 rpm for 5 min. For GSLM, *Chlorella* were collected by centrifugation after liquefaction at 4 °C. The collected *Chlorella* were washed three times with deionized water and then vacuum freeze-dried. Dried cells were immersed in 10 mL of 80% ethanol and stirred for 30 min in 80 °C water bath. Then, the mixture was centrifuged at 6000 rpm for 10 min to obtain supernatant. The residue was extracted three times with 80% ethanol, and supernatants were combined. The 1 mL extraction was added into the 5 mL anthrone test solution [anthrone (1 mg/mL)/80% H_2SO_4]. The mixture was boiled in a boiling bath for 10 min, and the absorbance at 625 nm (OD_{625})

was detected. The carbohydrate content was calculated via carbohydrate content–OD_{625} standard curve. The standard curve was protracted by treating a series of glucose solutions with the same method and measuring OD_{625}.

Measurement of protein content

For SSLM, *Chlorella* were collected by centrifugation at 6000 rpm for 5 min. For GSLM, *Chlorella* were collected by centrifugation after liquefaction at 4 °C. The collected *Chlorella* were washed 3 times with PBS solution (pH = 7.4), and then proteins were extracted by repeated alternating freezing and thawing cycles. Samples were centrifuged at 6000 rpm for 5 minutes and the supernatant collected. Protein content in *Chlorella* was determined spectrophotometrically using the BCA Protein Assay Kit (Biosharp, Beijing, China).

Measurement of lipid content

For SSLM, *Chlorella* were collected by centrifugation at 6000 rpm for 5 min. For GSLM, *Chlorella* were collected by centrifugation after liquefaction at 4 °C. The collected *Chlorella* were washed three times with deionized water and then vacuum freeze-dried. The dried cells were weighed (M_1) and immersed in diethyl ether for 16 hours, then extracted in a Soxhlet extractor for 8 hours. Samples were dried and weighed (M_2). The lipid content was calculated by the following equation:

$$\text{Lipid content (\%)} = (M_1 - M_2)/M_1 \times 100\% \quad (5)$$

Application demonstration of microalgae hydrogen fuel cell

The hydrogen-oxygen/air fuel cell (Generate voltage: 1.80 - 3.84 V/DC), small fan (Start current: 8 mA; Operating voltage range: 0.18 - 6.0 V.) and gas storage tank (30 mL) were provided by H-TEC education (USA). The quadrupole hydrogen-oxygen/air fuel cell had four reaction surfaces, and the electrode area was 14.4 cm^2. The fuel cell had four vent plugs. When the gas plug was closed and pure oxygen was introduced, the fuel cell was in the pure oxygen working mode (Output power: 2400-2600 mW/ 1.5 A); when the gas plug was pulled out, the fuel cell used the oxygen in the air to work and was in the air working mode (Output power: 720 - 800 mW/ 375 mA). The demonstration experiment adopted the air working mode. The photobioreactor for *Chlorella* was converted from a cell culture flask (300 mL). In this demonstration, we used 5 wt% copolymer and 6.51 $\times 10^6$ cells/mL *Chlorella* suspension to generate SSLM in a 300 mL microalgae photobioreactor. GSLM were generated when *Chlorella* proliferated to 1.73 $\times 10^8$ cells/mL. The photobioreactor was placed under the light intensity of 50 $\mu E \cdot m^{-2} \cdot s^{-1}$ for 4 days, and then the gas generated from the microalgae photoreactor was collected by drainage method. The water discharged from the upper layer of the gas storage tank was removed in time to avoid the adverse effect of water pressure on the hydrogen production of *Chlorella*. In 4 days, the gas storage tank collected about 7 ml of hydrogen with rates of 0.108 μmol H_2 (mg chlorophyll)$^{-1}$ h^{-1}. The gas storage tank, fuel cell and fan were connected after the hydrogen collection was complete. The speed control valve was opened, and water was added to the upper layer of the gas storage tank to squeeze the collected hydrogen into the fuel cell, and then the fuel cell worked to generate electricity to drive the fan to rotate.

Determination of gross photosynthetic rate of *Chlorella*

Two parts of 10 mL *Chlorella* were taken, and the oxygen content (Oc_1, μmol/L) in the *Chlorella* was measured with a dissolved oxygen meter. One was left untreated, and the other was wrapped in tin foil to avoid light treatment, and then both were placed in a light incubator at 20 °C/ 30 °C with a light intensity of 50 μE m^{-2} s^{-1}. One hour later, the oxygen content (Oc_2, μmol/L) in the untreated *Chlorella* and the oxygen content (Oc_3, μmol/L) in the *Chlorella*

treated in the dark were measured with a dissolved oxygen meter. Chlorophyll content in *Chlorella*: $Chlc_0$, mg/L.

Respiration rate (μmol O_2(mg chlorophyll)$^{-1}h^{-1}$) = (Oc_1- Oc_3)/ $Chlc_0$ (6)

Net photosynthetic rate (μmol O_2(mg chlorophyll)$^{-1}h^{-1}$) = (Oc_2- Oc_1)/ $Chlc_0$ (7)

Gross photosynthetic rate (μmol O_2(mg chlorophyll)$^{-1}h^{-1}$) = (Oc_2- Oc_3)/ $Chlc_0$ (8)

Average specific growth rate

The average specific growth rate of *Chlorella* was calculated by the following equation:

Average specific growth rates per day: n (day^{-1}) = (C_{n+1}-C_n) / (C_n × t) (9)

Where C_{n+1} was the algae concentration on day n+1; C_n was the algae concentration on day n; t was 1 day.

The average specific growth rate of free algae in SSLM and the average specific growth rate of algae encapsulated in GSLM (free algae were not included) were calculated, respectively.

Microsensor measurements

The H_2 microsensor was H210 microsensor (Unisense, Denmark) with a tip diameter of 10 μm. The O_2 microsensor was OX10 microsensor (Unisense, Denmark) with a tip diameter of 10 μm. After 24 h of light exposure (50 $\mu E \cdot m^{-2} \cdot s^{-1}$), the H_2 and O_2 concentrations in the *Chlorella* were detected by immersing the H_2 and O_2 microsensors in the suspension. H_2 and O_2 concentrations were detected by piercing the living material with H_2 and O_2 microelectrodes, respectively. A layer of agar matrix (5 mm) was spread under the object to be measured to avoid breakage of the microsensors. In order to obtain stable and reliable results, the living material was transferred to agar to equilibrate for 1 hour under the light intensity of 50 $\mu E \cdot m^{-2} \cdot s^{-1}$, and then the experiment was carried out. The micromanipulation step size was 50 μm.

Statistical analysis

All experiments were repeated at least 3 times as independent experiments, and results were reported as mean ± SD. A two-tailed, Student's t test was used for testing the significance between two groups. A one-way analysis of variance (ANOVA) with Dunnett's test was performed to test the significance for multiple comparisons. Statistical significance was indicated as *P < 0.05, **P < 0.01, ***P < 0.001, and ****P < 0.0001. No data were excluded from the analysis. Samples were randomly assigned to different experimental groups. Organisms were cultured and maintained in the same environment and randomly assigned to each group. Investigators were not blinded during data collection and analysis.

Supporting Figures

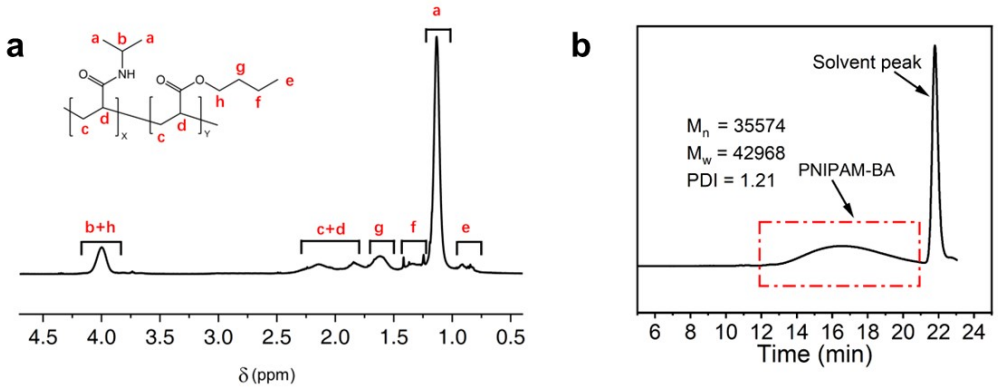

Figure S1. a ^{1}H NMR spectrum for PNIPAM-BA in $CDCl_3$. The spectrum confirmed successful synthesis of the polymer. In ^{1}H NMR, a very shielded 0.89 ppm peak (e) with low integration represents the methyl proton at the end of the carbon chain. The isopropylmethyl peak (a) is not well resolved, lacking a baseline and suggesting overlap with other peaks. This requires comparing the low field peak at 3.96 ppm (b+h), representing protons deshielded by electronegative atoms, to the butyl acrylate methyl peak (e) as a measure of the accuracy of the feed ratio. The copolymer composition calculated from the ^{1}H NMR spectrum is close to stoichiometric, indicating that the feed ratio (NIPAM : BA = 95:5) is relatively accurate. **b** GPC molecular weight distributions of PNIPAM-BA sample by using DMF as mobile phase. Mn = 35600 g/mol; Mw = 43000 g/mol; PDI = 1.21. This test result only represented the relative molar mass of PNIPAM-BA and not the absolute molar mass.

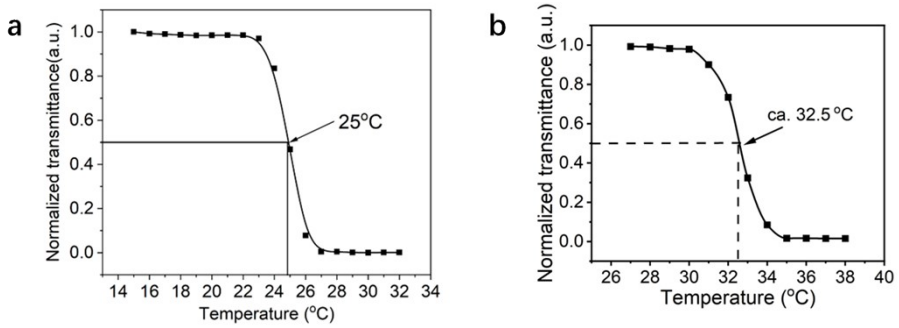

Figure S2. a Variation in transmittance of 0.1 wt% PNIPAM-BA suspension. The lower critical solution temperature (LCST) (approximately 25 °C) was determined as the midpoint of the region of the sharp increase in extinction of the suspension, caused by the strong light scattering by PNIPAM-BA aggregates. **b** Variation in transmittance of 0.1 wt% PNIPAM suspension. The lower critical solution temperature (LCST) (approximately 32.5 °C) was determined as the midpoint of the region of the sharp increase in extinction of the suspension, caused by the strong light scattering by PNIPAM aggregates.

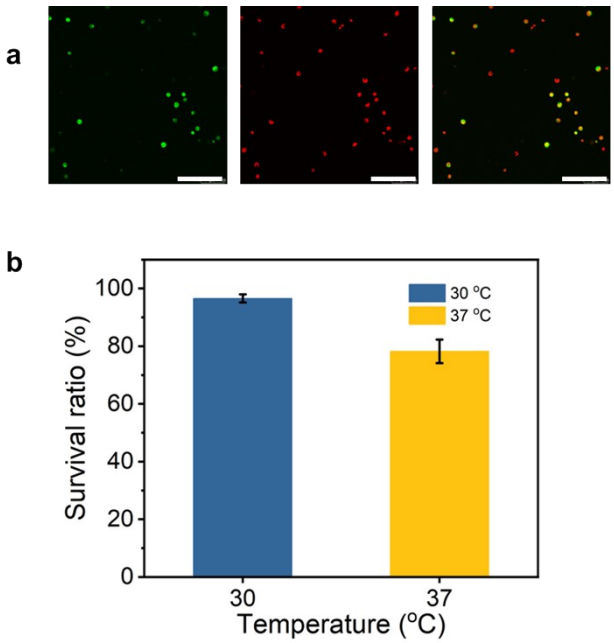

Figure S3. a CLSM images of algae incubated at 37 °C for 24 hours. The green fluorescence was from viable *Chlorella* and the red fluorescence was from intracellular chlorophyll. Scale bars, 50 μm. **b** *Chlorella* survival ratio at 30 °C and 37 °C for 24 hours, respectively. *Chlorella* survival ratio was calculated by dividing the number of green fluorescent *Chlorella* by the number of red fluorescent *Chlorella* (n = 3, means ± SD).

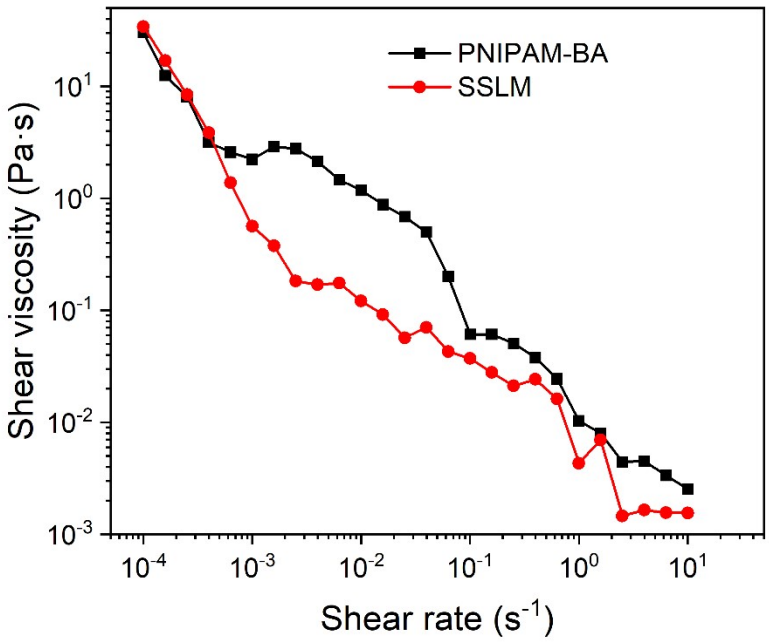

Figure S4. Variation in shear viscosity of SSLM and PNIPAM-BA alone at 20 °C as a function of shear rate. There was no significant difference in shear viscosity between SSLM and PNIPAM-BA, and shear thinning was observed for both.

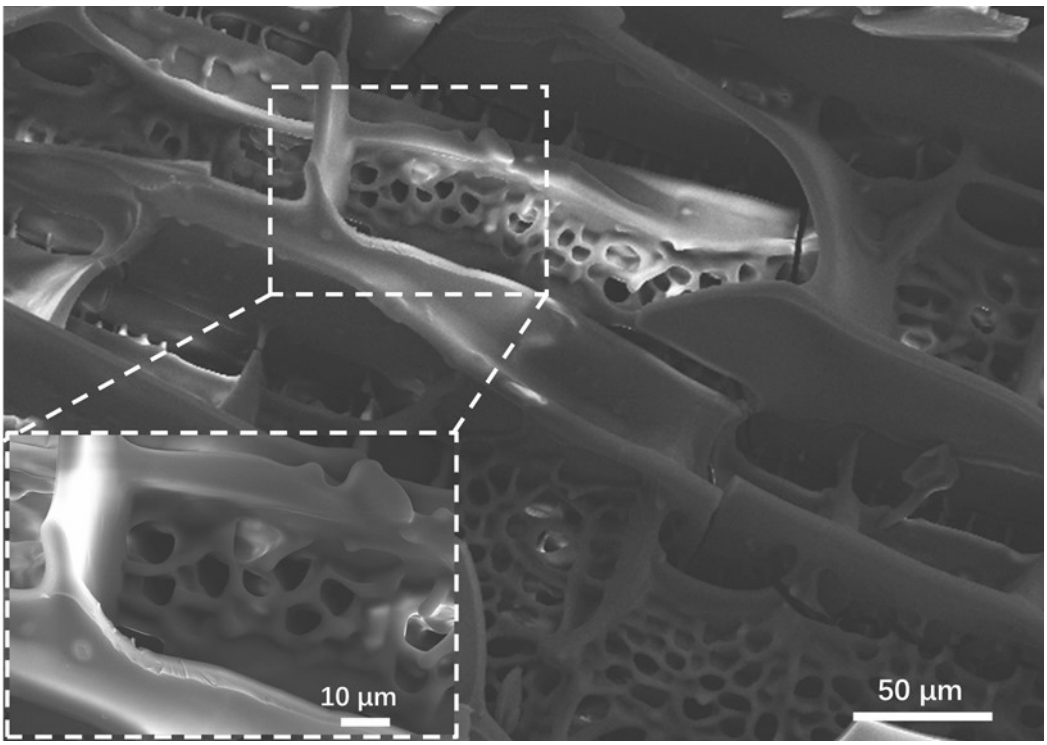

Figure S5. SEM image of GSLM obtained by placing SSLM in a 30 °C water bath for 1 minute. Scale bar, 50 µm. Inset showed a partially magnified SEM image. Scale bar, 10 µm.

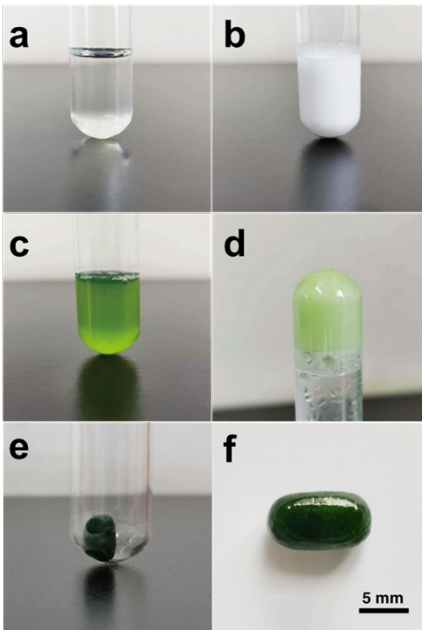

Figure S6. Images of PNIAPAM-BA suspension at 20 °C (**a**) and 30 °C (**b**), respectively. Images of *Chlorella* and PNIAPAM-BA mixed suspension at 20 °C (**c**) and 30 °C (**d**), respectively. **e** GSLM was prepared by placing sol-state living material SSLM at 30 °C for 2 hours (*Chlorella* concentration of 7.55×10^7 cells/mL and PNIPAM-BA concentration of 5 wt%). **f** Image of rod-shaped GSLM. Scale bar, 5mm.

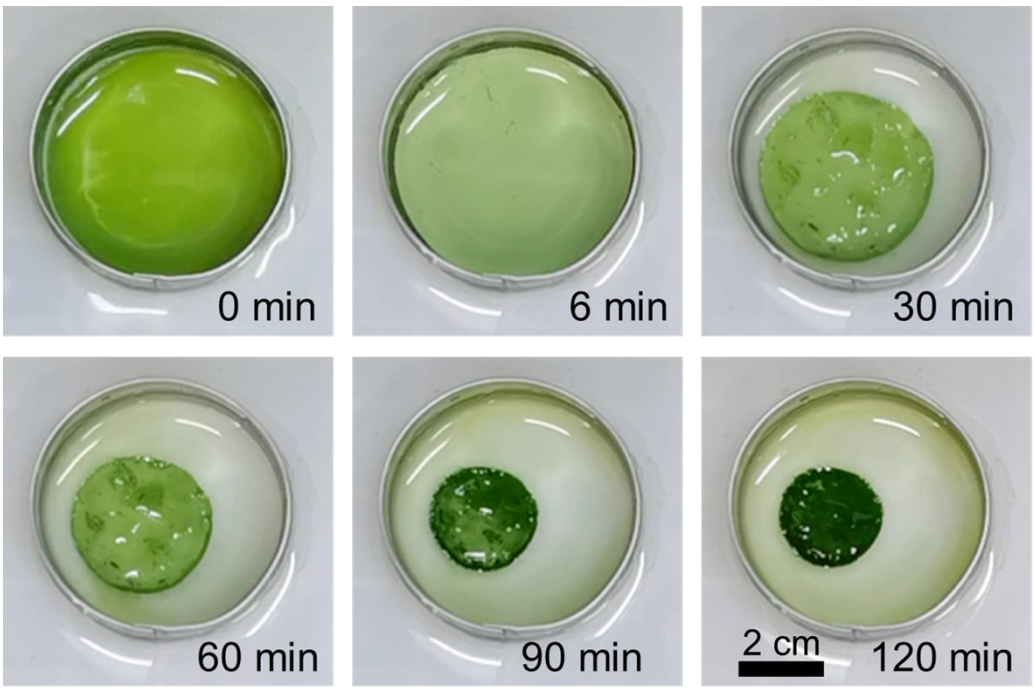

Figure S7. Time-series pictures of the transformation of SSLM into GSLM at 30 °C (*Chlorella* concentration of 7.55 ×10^7 cells/mL and PNIPAM-BA concentration of 5 wt%). The living material became opaque and volume shrinkage were clearly observed.

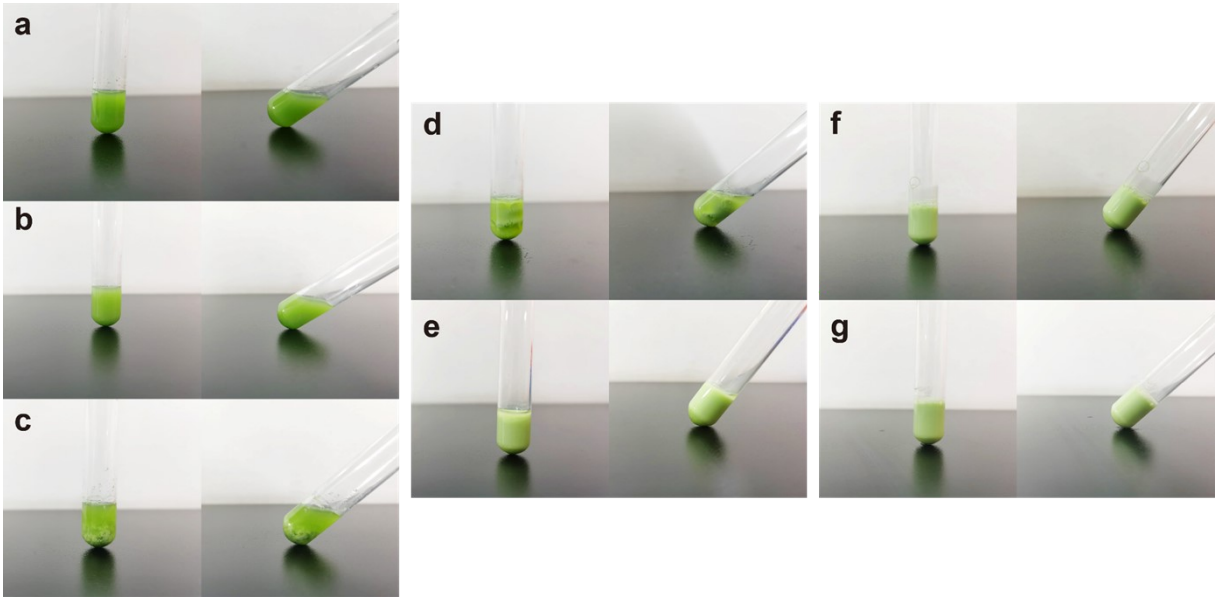

Figure S8. Pictures of PNIPAM-BA at concentrations 0.5 wt% (a), 1 wt% (b), 2.5 wt% (c), 3.75 wt% (d), 5 wt% (e), 10 wt% (f) and 15 wt% (g) mixed with *Chlorella* suspension (7.55 $\times 10^7$ cells/mL) heated to 30 °C.

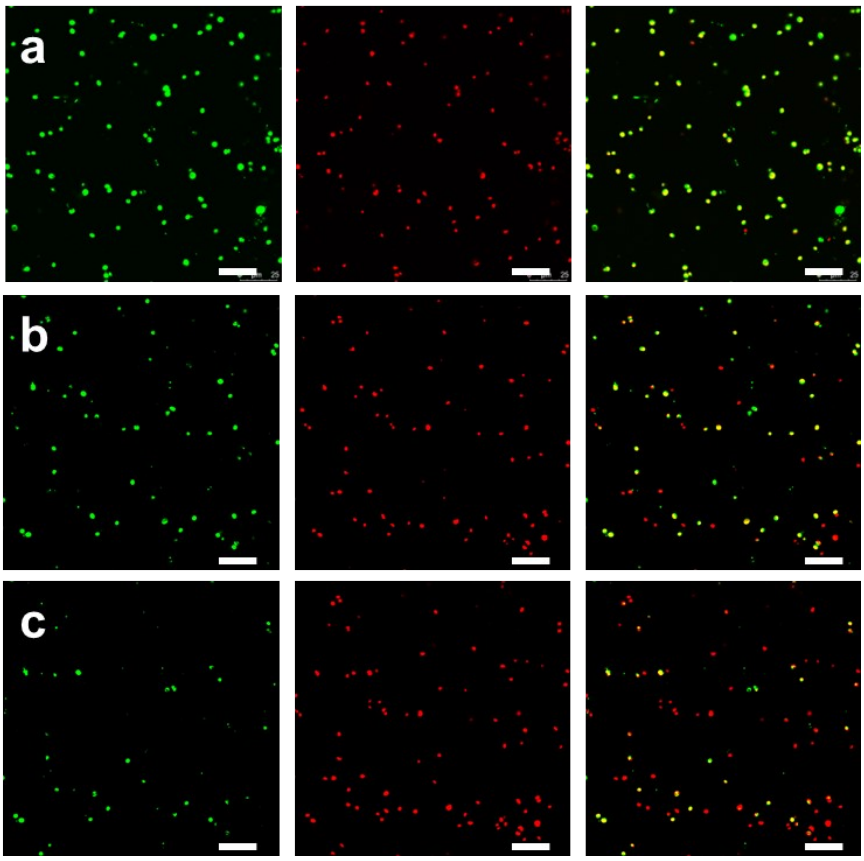

Figure S9. CLSM images of the effect of SSLM formed with different concentrations of PNIPAM-BA (5 wt% (a), 7 wt% (b), 10 wt% (c)) on the activity of *Chlorella* after 24 hours. The green fluorescence was from viable *Chlorella* and the red fluorescence was from intracellular chlorophyll. Scale bars, 25 μm.

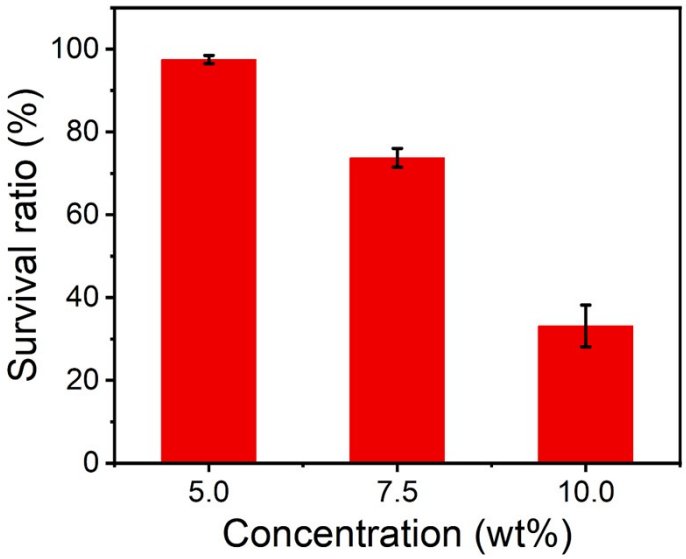

Figure S10. *Chlorella* survival ratio within 24 hours in SSLM at 5 wt%, 7.5 wt%, 10 wt% PNIAPM-BA concentrations, respectively. *Chlorella* survival ratio was calculated by dividing the number of green fluorescent *Chlorella* by the number of red fluorescent *Chlorella* (n = 3, means ± SD).

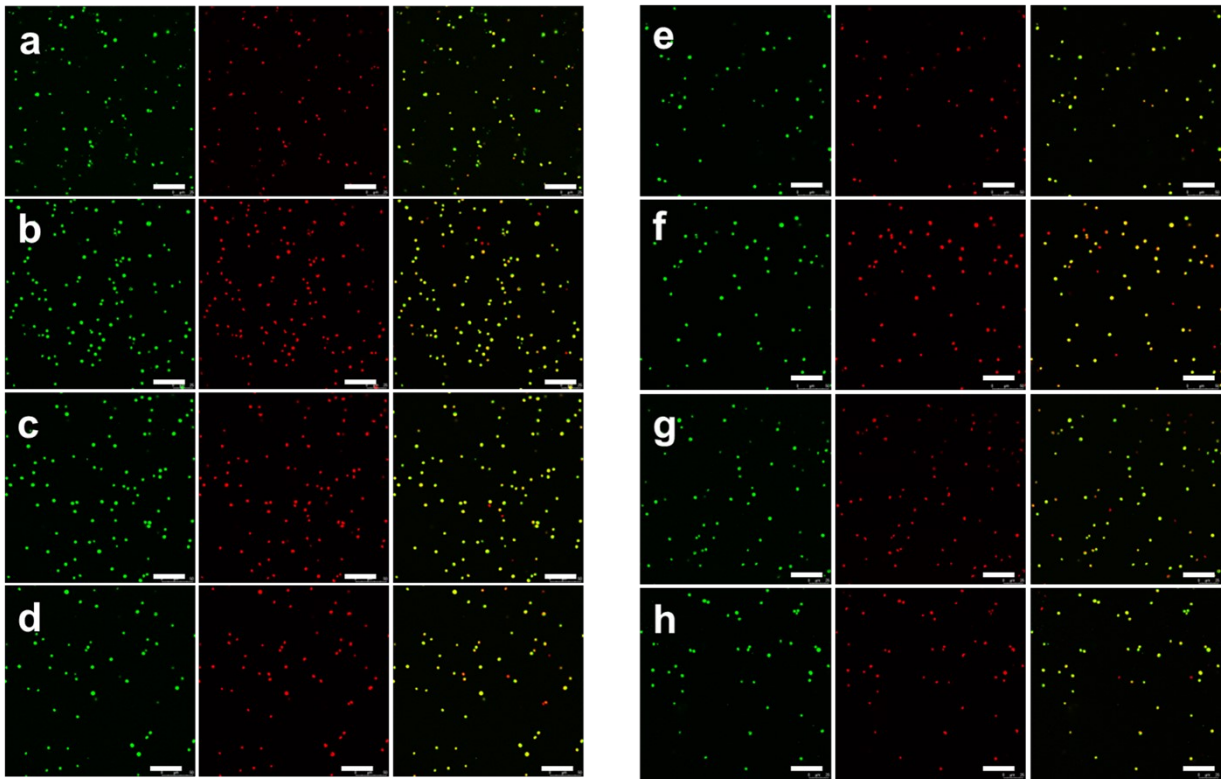

Figure S11. CLSM images for monitoring *Chlorella* activity in BG-11 solution for 7 days. (a) to (h) represented day 0 to day 7, respectively. The green fluorescence was from viable *Chlorella* and the red fluorescence was from intracellular chlorophyll. Scale bars, 25 μm.

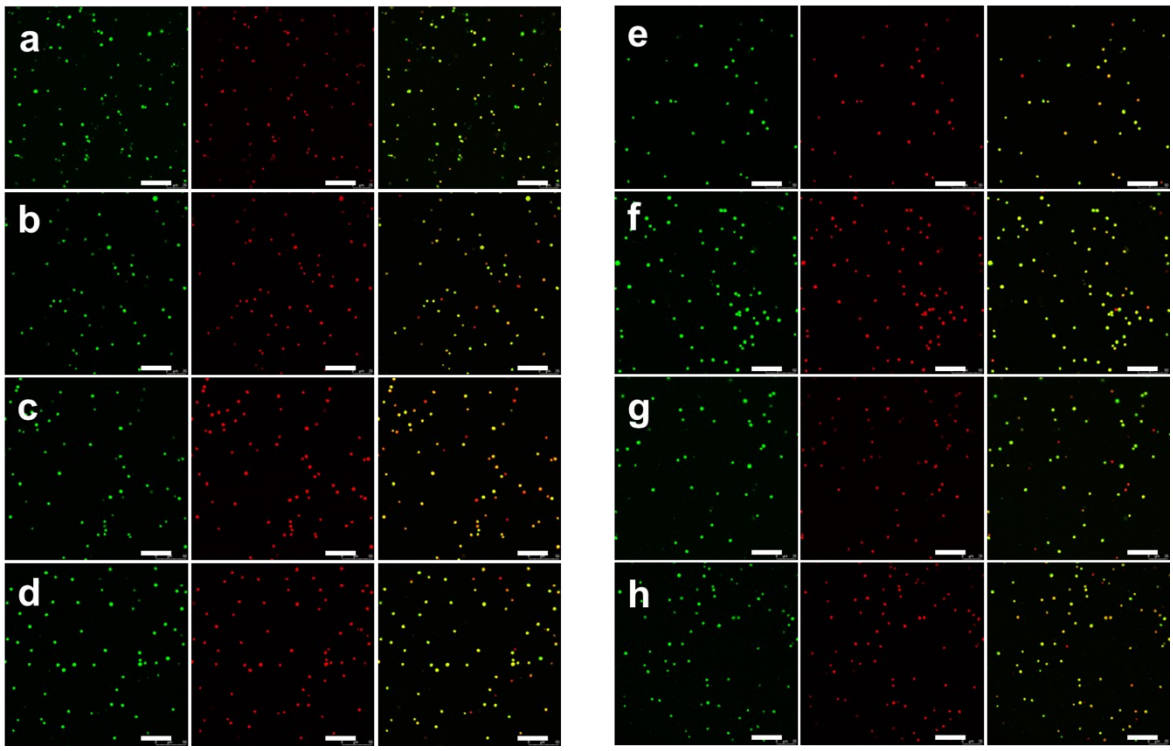

Figure S12. CLSM images for monitoring *Chlorella* activity in GSLM for 7 days. (a) to (h) represented day 0 to day 7, respectively. The green fluorescence was from viable *Chlorella* and the red fluorescence was from intracellular chlorophyll. Scale bars, 25 μm.

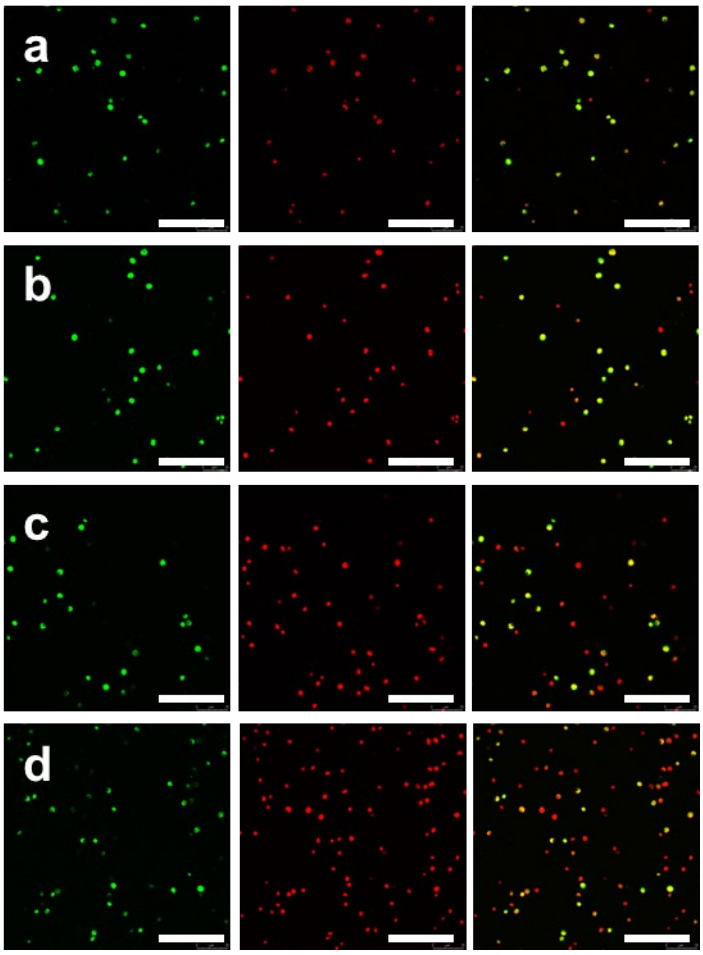

Figure S13. CLSM images for monitoring *Chlorella* activity in GSLM. (a), (b), (c) and (d) represented day 5, day 10, day 15 and day 20, respectively. The green fluorescence was from viable *Chlorella* and the red fluorescence was from intracellular chlorophyll. Scale bars, 50 μm.

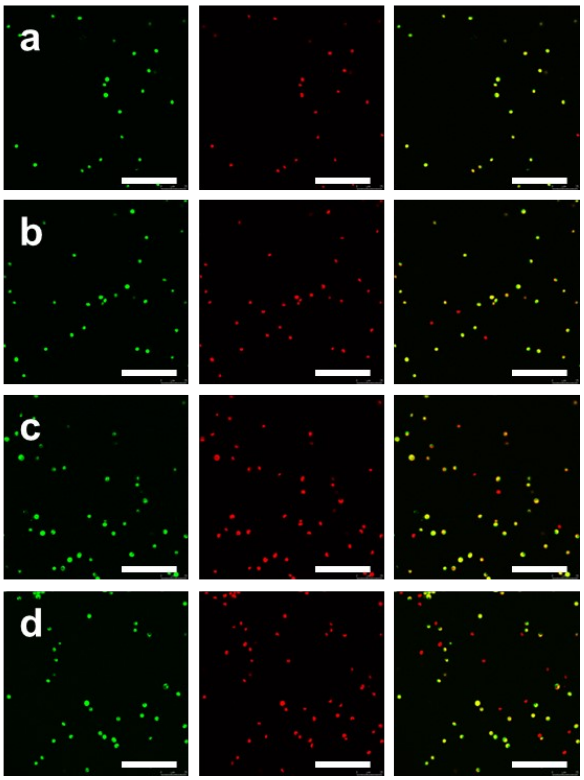

Figure S14. CLSM images for monitoring *Chlorella* activity in BG-11 solution. (a), (b), (c) and (d) represented day 5, day 10, day 15 and day 20, respectively. The green fluorescence was from viable *Chlorella* and the red fluorescence was from intracellular chlorophyll. Scale bars, 50 μm.

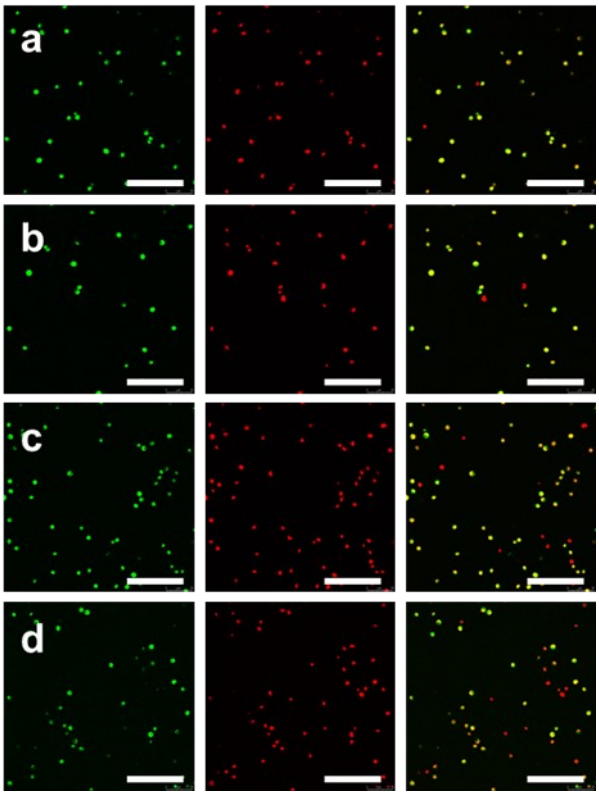

Figure S15. CLSM images for monitoring *Chlorella* activity in SSLM. (a), (b), (c) and (d) represented day 5, day 10, day 15 and day 20, respectively. The green fluorescence was from viable *Chlorella* and the red fluorescence was from intracellular chlorophyll. Scale bars, 50 μm.

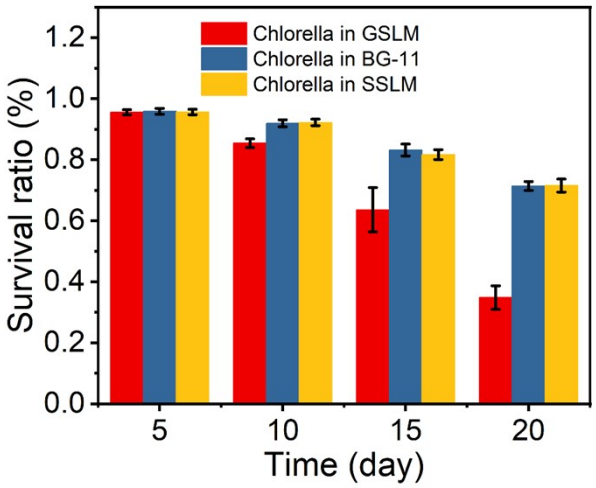

Figure S16. Survival ratios of *Chlorella* on day 5, 10, 15 and 20 in SSLM, BG-11 and GSLM (n = 3, means ± SD). *Chlorella* survival ratio was calculated by dividing the number of green fluorescent *Chlorella* by the number of red fluorescent *Chlorella*. The survival ratios of *Chlorella* in GSLM on day 5, day 10, day 15 and day 20 were 95.6%, 85.4%, 63.6%, 34.8%, respectively. In BG-11, the survival ratios of *Chlorella* on day 5, day 10, day 15 and day 20 were 95.9%, 91.9%, 83.2%, 71.4%, respectively. In SSLM, the survival ratios of *Chlorella* on day 5, day 10, day 15 and day 20 were 95.6%, 92.2%, 81.7%, 71.5%, respectively. No significant difference was observed in the survival ratio of *Chlorella* between BG-11 and SSLM. *Chlorella* survival decreased in BG-11 and SSLM due to depletion of media nutrients. The reason for the rapid decline of *Chlorella* survival ratio in GSLM was the depletion of organic matter in *Chlorella* and the influence of shading effect.

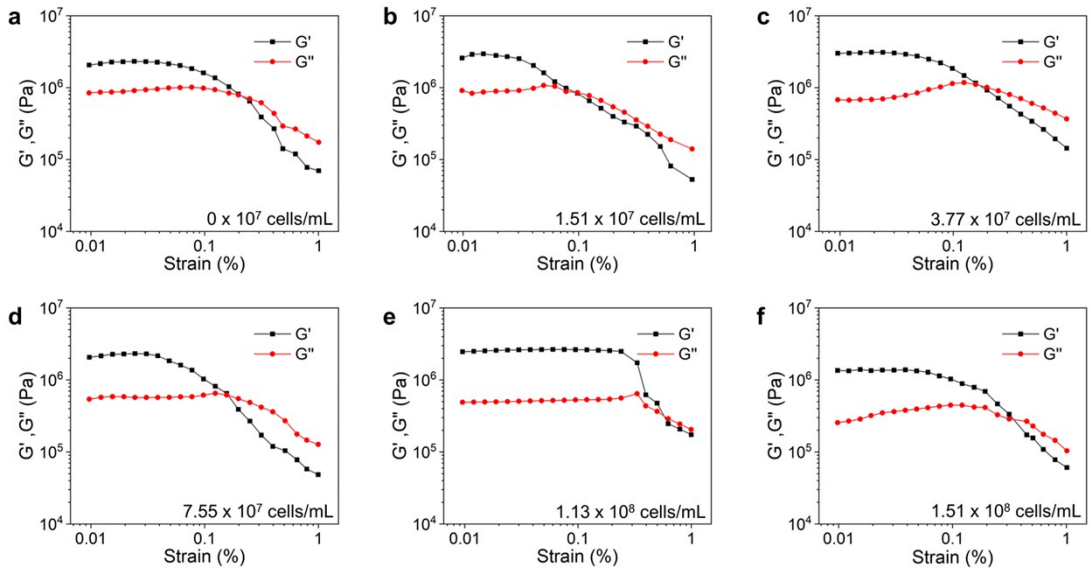

Figure S17. Variation in storage modulus (G', black squares) and loss modulus (G", red circles) in strain-sweep experiments conducted for GSLM with different *Chlorella* concentrations from 0 to 1.51 $\times 10^8$ cells/mL at 30 °C. At < 0.05% strain, a linear viscoelastic response of the living material was observed. At > 0.1% strain, the living material exhibited nonlinear viscoelastic behavior, and beyond the yield strain, the disruption of the physical cross-linked network caused both G' and G" to decrease along with the increased strain.

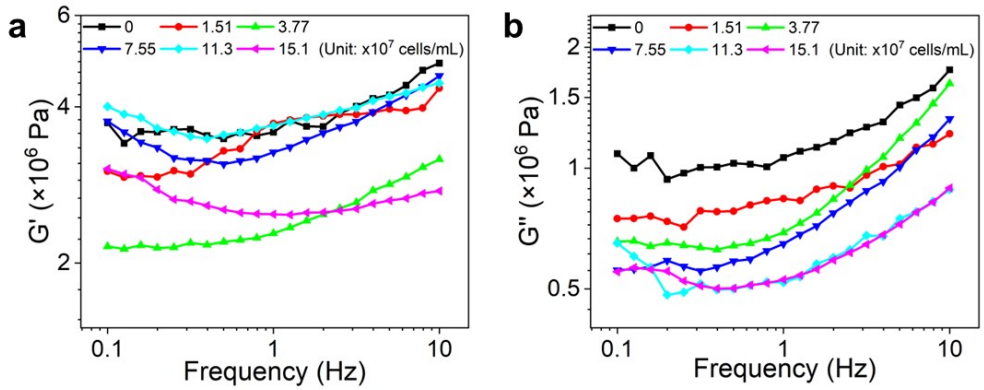

Figure S18. Variation in storage modulus (a) and loss modulus (b) in frequency-sweep experiments conducted for GSLM with different *Chlorella* concentrations from 0 to 1.51 $\times 10^8$ cells/mL at 30 °C. The G' and G'' of the GSLM formed by different concentrations of *Chlorella* ranging from 2.13 to 4.86 MPa and 0.48 to 1.76 MPa, respectively.

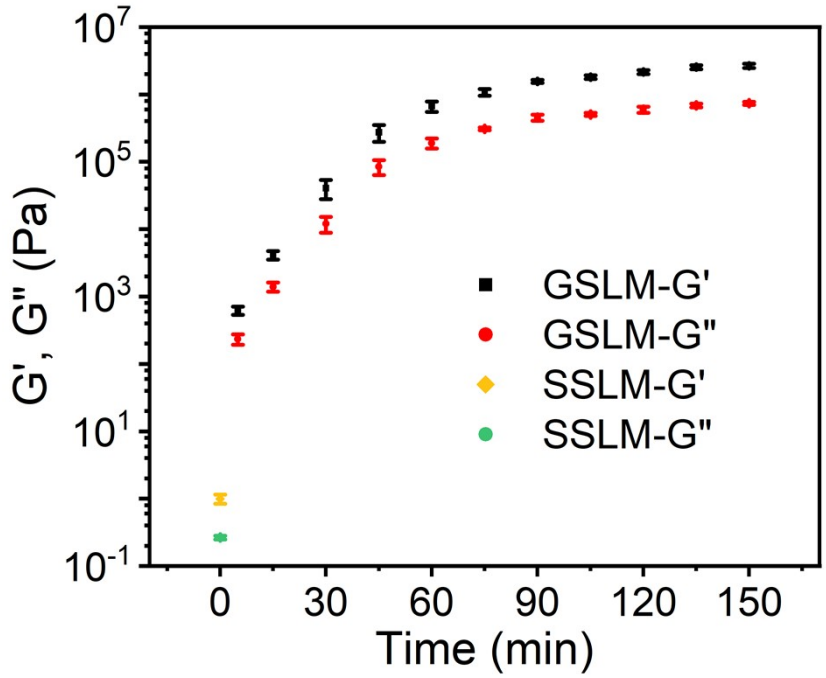

Figure S19. Variation in storage modulus and loss modulus in time-sweep experiments conducted for living material with *Chlorella* concentration of 7.55 $\times 10^7$ cells/mL and PNIPAM-BA concentration of 5 wt% (n = 3, means ± SD).

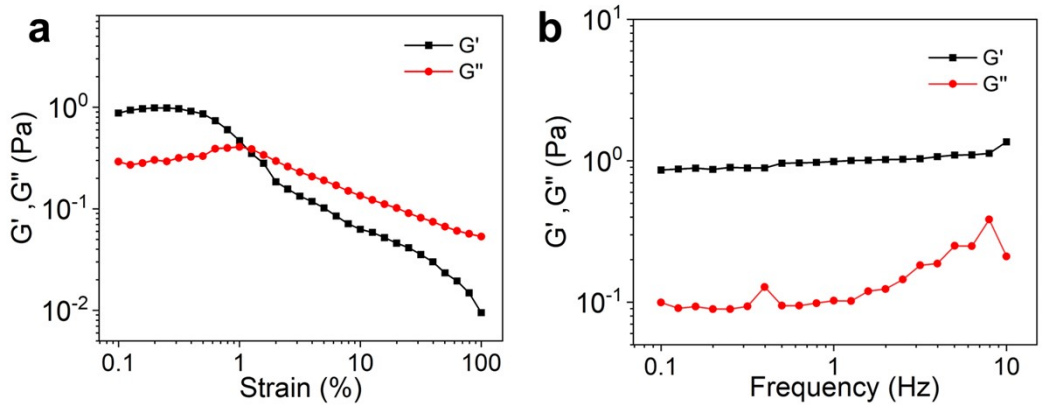

Figure S20. Variation in storage modulus and loss modulus in strain-sweep (a) and frequency-sweep (b) experiments conducted for SSLM with *Chlorella* concentration of 7.55 $\times 10^7$ cells/mL and PNIPAM-BA concentration of 5 wt% at 20 ^{o}C.

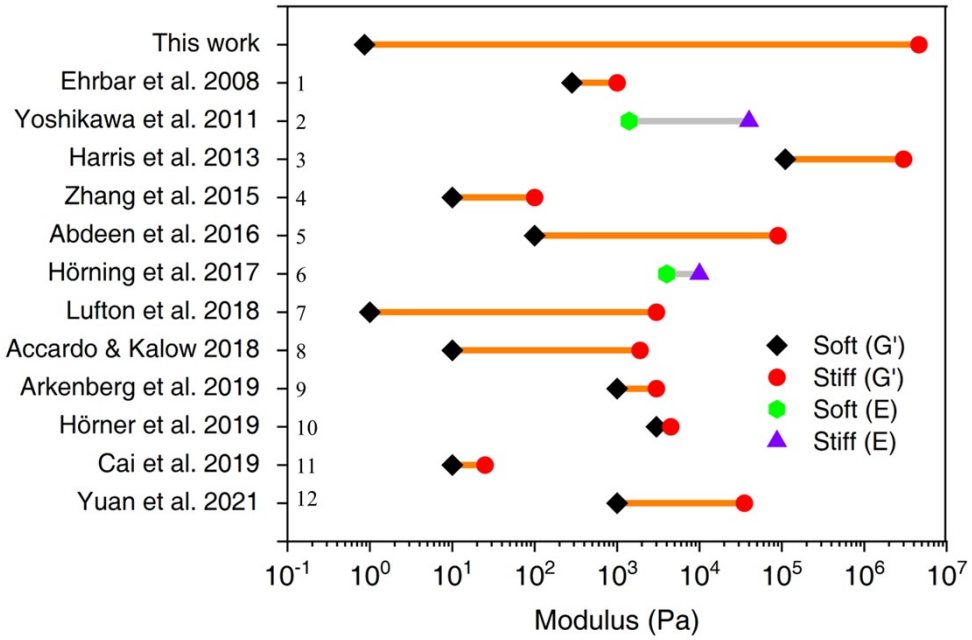

Figure S21. Storage modulus (G') or Young's modulus (E) of materials with tunable moduli between soft and stiff states existing in the literature. The living material composed of 7.55 $\times 10^7$ cells/mL of *Chlorella* and 5 wt% of PNIPAM-BA demonstrated a rather large tuning range of elastic modulus between 0.86 Pa and 4.59 MPa.

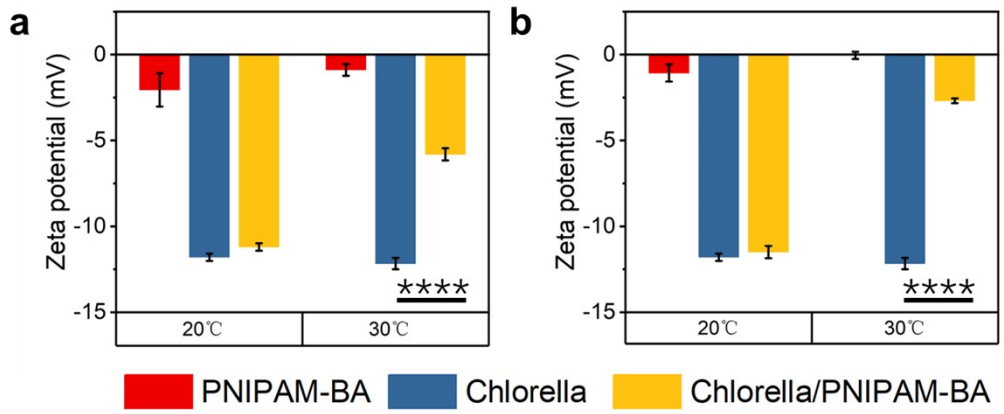

Figure S22. Zeta potentials of PNIPAM-BA, *Chlorella*, *Chlorella*/PNIPAM-BA at 20 °C and 30 °C with different PNIPAM-BA concentrations ((a) 0.025 wt%, (b) 0.05 wt%) (n = 3, means ± SD).

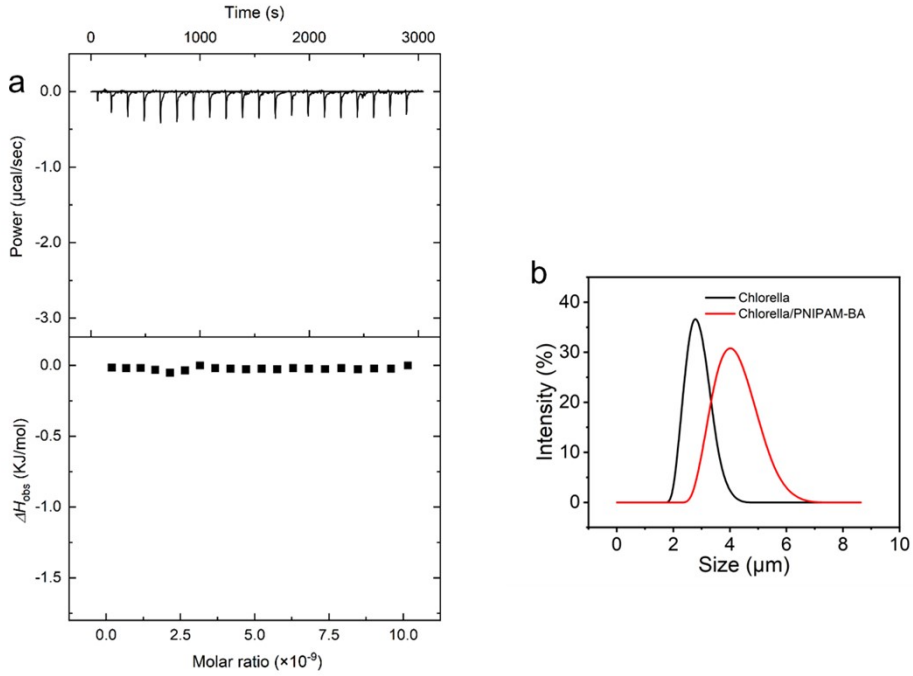

Figure S23. a ITC results of raw and integrated data of released heat for titration of *Chlorella* suspension to PNIPAM-BA solution at 20 °C. No significant titration enthalpy signal was observed. **b** Particle size distribution of *Chlorella* and *Chlorella*/PNIPAM-BA was measured using dynamic light scattering. PNIPAM-*co*-BA was bound to *Chlorella* and the particle size increased from 2.7 µm to 4.1 µm at 30 °C.

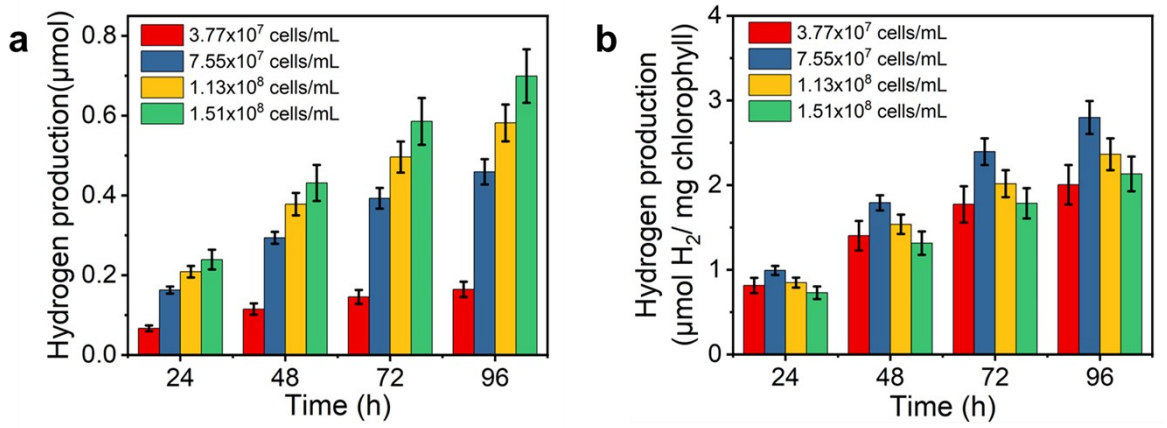

Figure S24. a The amount of hydrogen production from GSLM with different *Chlorella* contents from 3.77 $\times 10^7$ to 1.51 $\times 10^8$ cells/mL at 30 °C. Hydrogen production from GSLM increased with increasing concentrations of encapsulated *Chlorella* (n = 3, means ± SD). **b** The amount of hydrogen production from GSLM based on chlorophyll concentration with different *Chlorella* contents from 3.77 $\times 10^7$ to 1.51 $\times 10^8$ cells/mL at 30 °C. The *Chlorella* concentration of 7.55 $\times 10^7$ cells/mL had the highest hydrogen production based on the chlorophyll concentration. (n = 3, means ± SD).

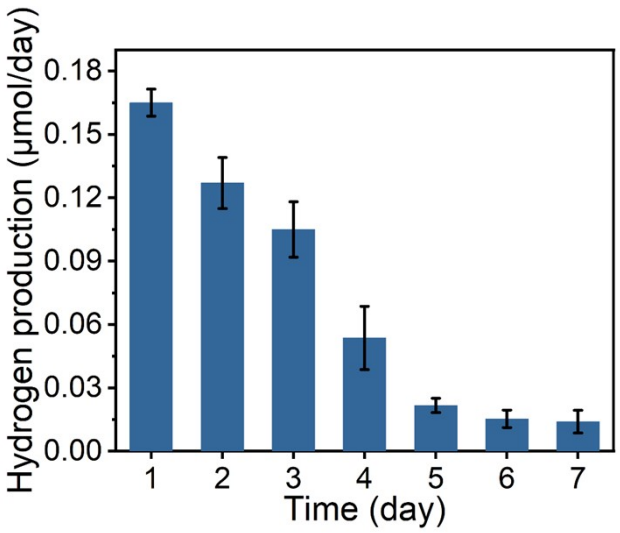

Figure S25. Average daily hydrogen production rates of microalgae in GSLM with BG-11 solution at 30 °C (n = 3, means ± SD).

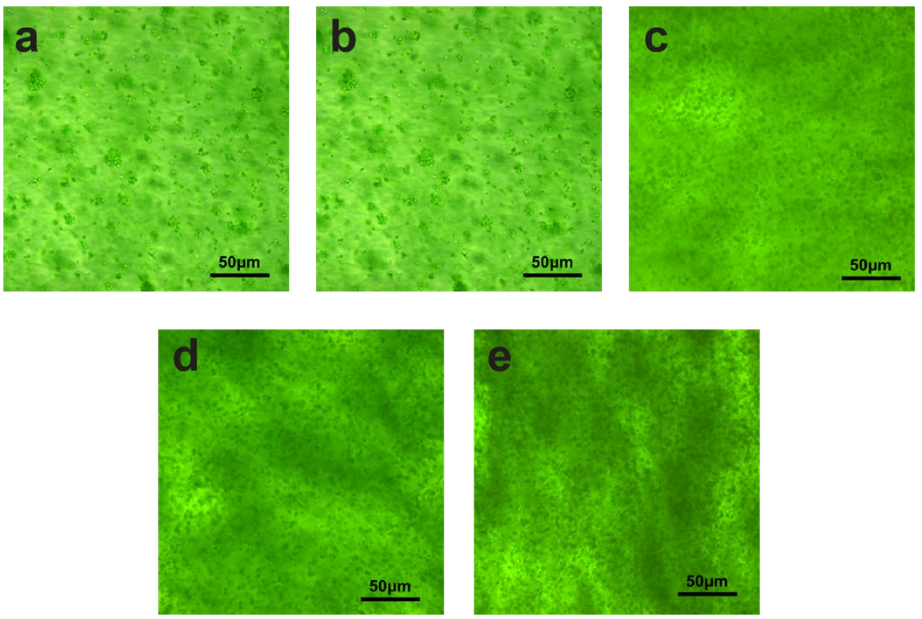

Figure S26. Optical microscope images of GSLM with different *Chlorella* concentrations ((a) 1.51 $\times 10^7$ cells/ml, (b) 3.77 $\times 10^7$ cells/ml, (c) 7.55 $\times 10^7$ cells/ml, (d) 1.13 $\times 10^8$ cells/ml, (e) 1.51 $\times 10^8$ cells/ml) and pnipam-ba concentration of 5 wt%. Scale bars, 50 μm.

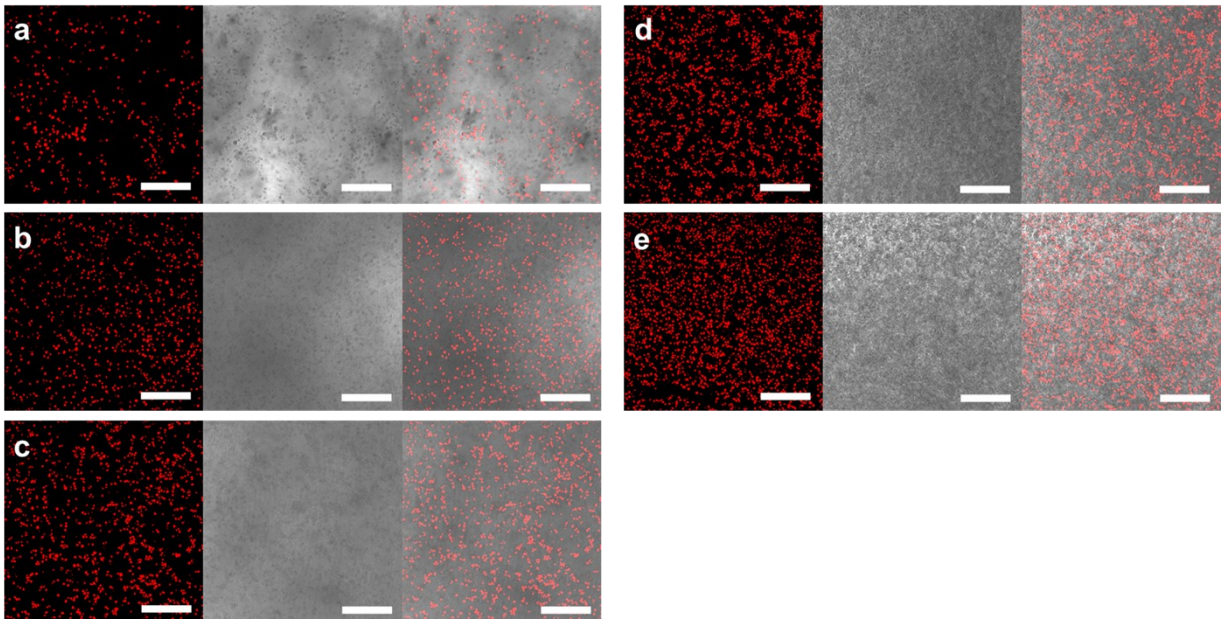

Figure S27. CLSM images of GSLM with different *Chlorella* concentrations ((a)1.51 $\times 10^7$ cells/ml, (b) 3.77 $\times 10^7$ cells/ml, (c) 7.55 $\times 10^7$ cells/ml, (d) 1.13 $\times 10^8$ cells/ml, (e) 1.51 $\times 10^8$ cells/mL) and PNIPAM-BA concentration of 5 wt%. Scale bars, 50 μm.

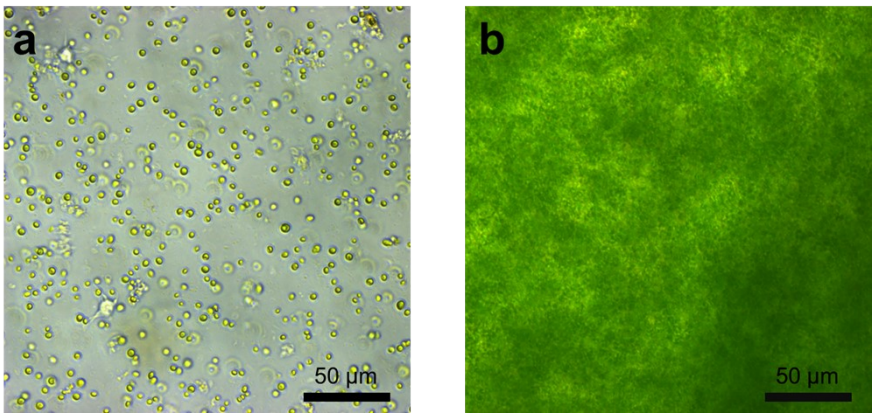

Figure S28. Optical microscope images of SSLM (a) and GSLM (b) with *Chlorella* concentration of 7.55 $\times 10^7$ cells/mL and PNIPAM-BA concentration of 5 wt%. Scale bars, 50 μm.

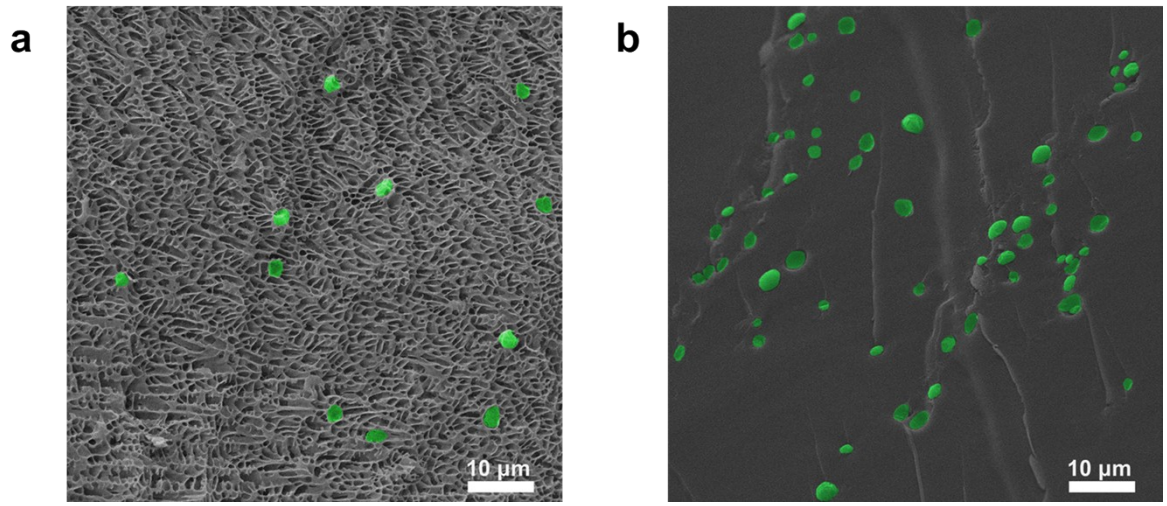

Figure S29. Cryo-SEM images of SSLM (a) and GSLM (b) with *Chlorella* concentration of 7.55 $\times 10^7$ cells/mL and PNIPAM-BA concentration of 5 wt%, where *Chlorella* were shown in pseudo-color. Scale bar, 10 μm. There were 11 *Chlorella* cells in the SSLM cryo-SEM image and 58 *Chlorella* cells in the GSLM cryo-SEM image. Within a unit section, the density of *Chlorella* increased by 5.27 times.

In SSLM, the concentration of *Chlorella* is 7.55 $\times 10^7$ cells/mL, that is, an average of one *Chlorella* cell occupies space of 1.325 $\times 10^4$ μm^3 and the distance between two *Chlorella* is about 23.66 μm. In GSLM, the concentration of *Chlorella* is 6.84 $\times 10^8$ cells/mL, that is, an average of one *Chlorella* cell occupies space of 1.462 $\times 10^3$ μm^3 and the distance between two *Chlorella* is about 11.35 μm. The real size of the cryo-SEM image of SSLM is 75.03 μm $\times$75.03 μm. Theoretically, there should be $75.03^2/23.66^2 = 10$ *Chlorella* cells on a cryo-SEM image of this size. In fact, there are 11 *Chlorella* cells in the cryo-SEM image of SSLM, which is almost in line with the theoretical prediction. According to similar calculations, in theory, the cryo-SEM image of GSLM should hold 44 *Chlorella* cells. And there are 58 *Chlorella* cells in reality, which is also close to the theoretical result.

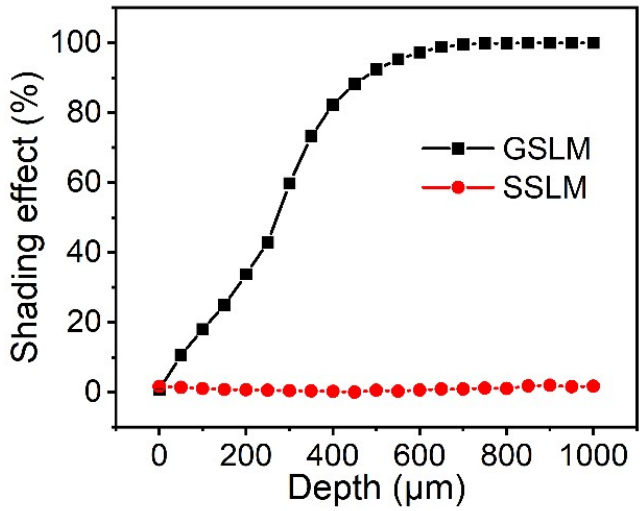

Figure S30. Shading effect as a function of microprobe insertion depth into SSLM (red circles) and GSLM (blank squares) (n = 3, means ± SD). Chlorella in SSLM experienced nearly zero shading effect within the depth range of 0-1000 μm, while in GSLM, the shading effect on microalgae increased with probe insertion reflected by the decrease of oxygen concentration, with the maximum effect occurring beyond the depth of 650 μm.

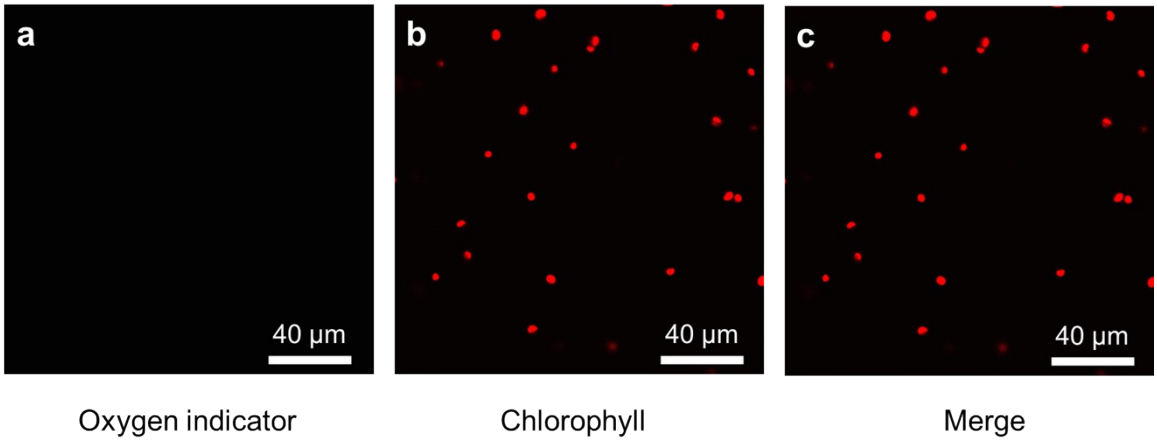

Figure S31. a No fluorescence was observed in *Chlorella* in the SSLM using the oxygen indicator $[Ru(dpp)_3]Cl_2$. The fluorescence of the dye was quenched under aerobic conditions, which indicated that the *Chlorella* in the SSLM were in an aerobic state. **b** The red fluorescence was from intracellular chlorophyll. **c** The merge of (a) and (b). Scale bar, 40 μm.

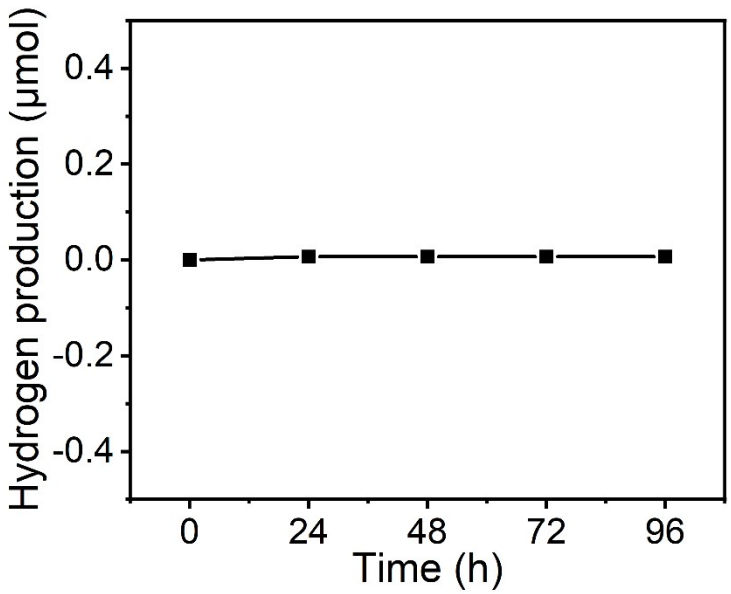

Figure S32. The amount of hydrogen production from the SSLM (*Chlorella* concentration of 7.55 ×10^7 cells/mL and PNIPAM-BA concentration of 5 wt%) at different time periods (n = 3, means ± SD). No hydrogen production was detected.

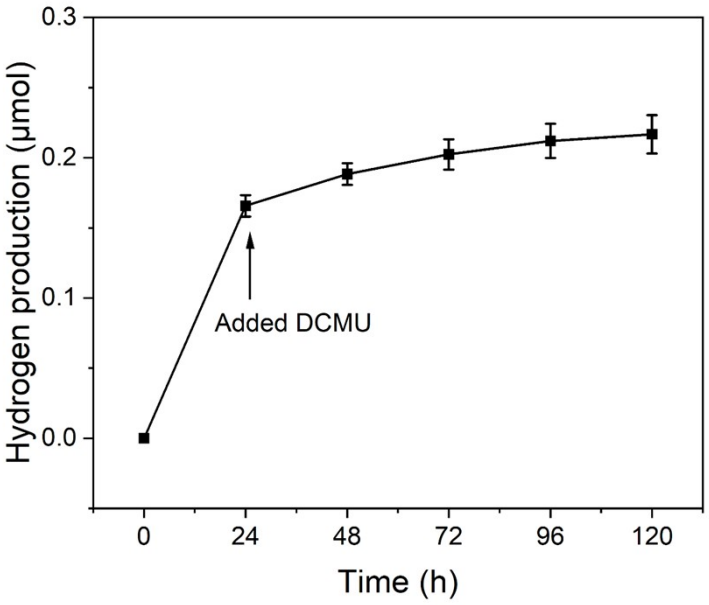

Figure S33. The effect on the H_2 production of GSLM (*Chlorella* concentration of 7.55 ×10^7 cells/mL and PNIPAM-BA concentration of 5 wt%) after adding DCMU (40 μL) into the solution (n = 3, means ± SD).

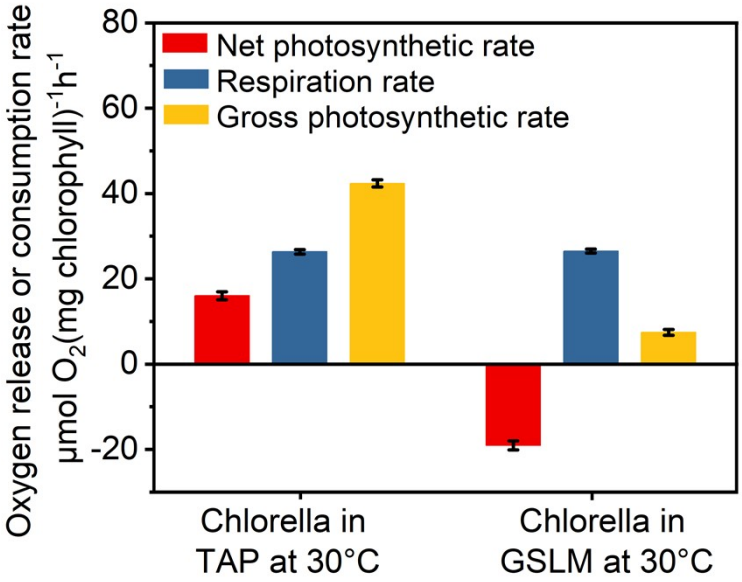

Figure S34. Net photosynthetic rate (red), respiration rate (blue) and gross photosynthetic rate (yellow) of *Chlorella* in TAP at 30 °C and in GSLM at 30 °C respectively (n =3, means ± SD).

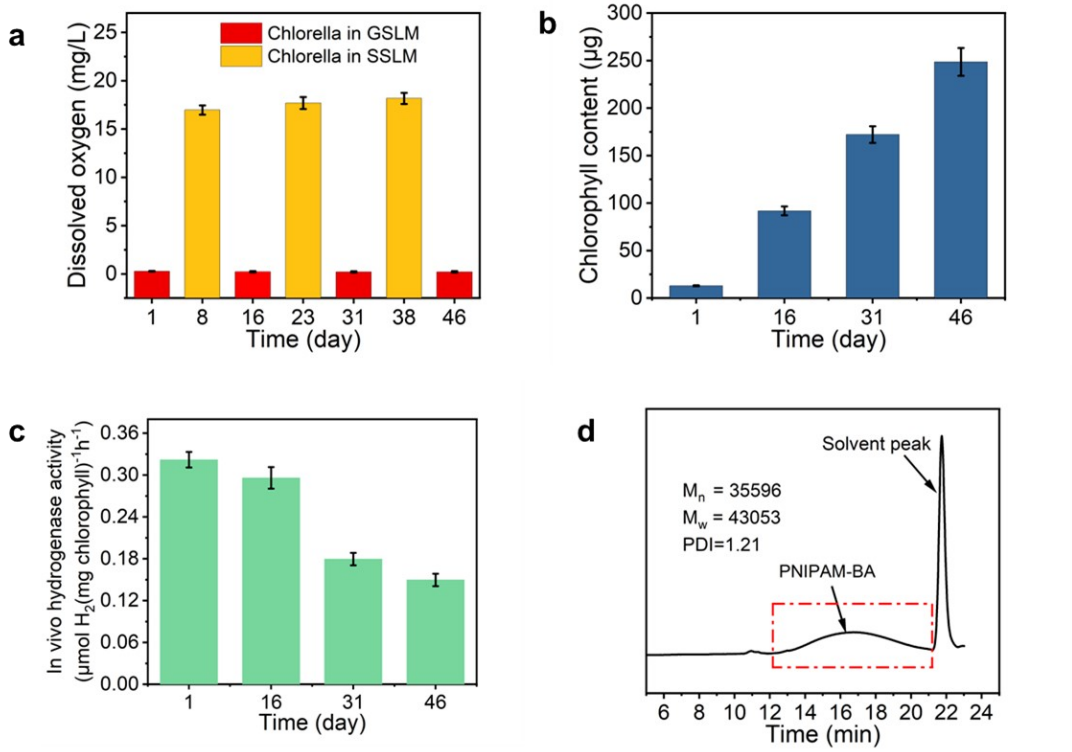

Figure S35. Dissolved oxygen concentration (**a**), total amount of chlorophyll (**b**), and hydrogenase activity data (**c**) in the 45-day experiment. **d** GPC was used to determine the relative molar mass of PNIPAM-BA on day 45. Mn = 35600 g/mol; Mw = 43000 g/mol. This test result only represented the relative molar mass of PNIPAM-BA and not the absolute molar mass. The relative molecular weight of PNIPAM-BA was not found to decrease, which indicated that PNIPAM-BA was not decomposed by algae.

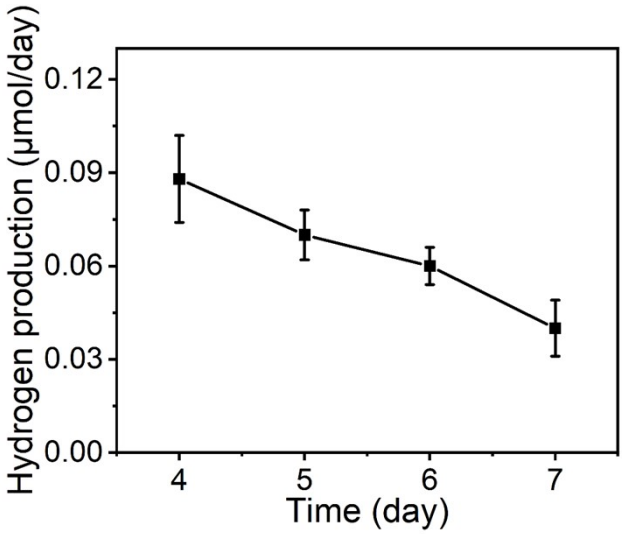

Figure S36. The rate of hydrogen production from the GSLM (*Chlorella* concentration of 7.55×10^7 cells/mL and PNIPAM-BA concentration of 5 wt%) at 30 °C in TAP solution from day 4 to 7 (n = 3, means ± SD).

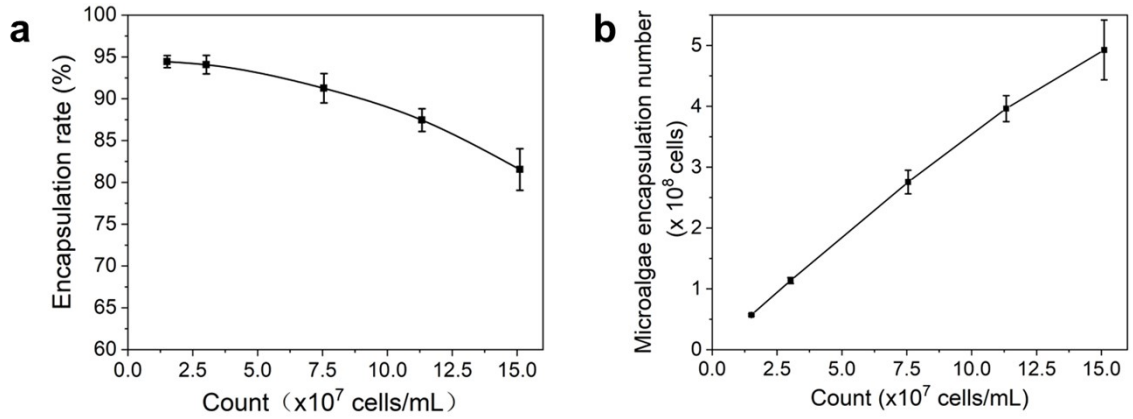

Figure S37. a Variation curve of microalgae encapsulation rate of GSLM with different *Chlorella* concentrations from 1.51 ×10^7 cells/mL to 1.51 ×10^8 cells/mL (n = 3, means ± SD). **b** Variation curve of microalgae encapsulation number of GSLM with different *Chlorella* concentrations from 1.51 ×10^7 cells/mL to 1.51 ×10^8 cells/mL (n = 3, means ± SD).

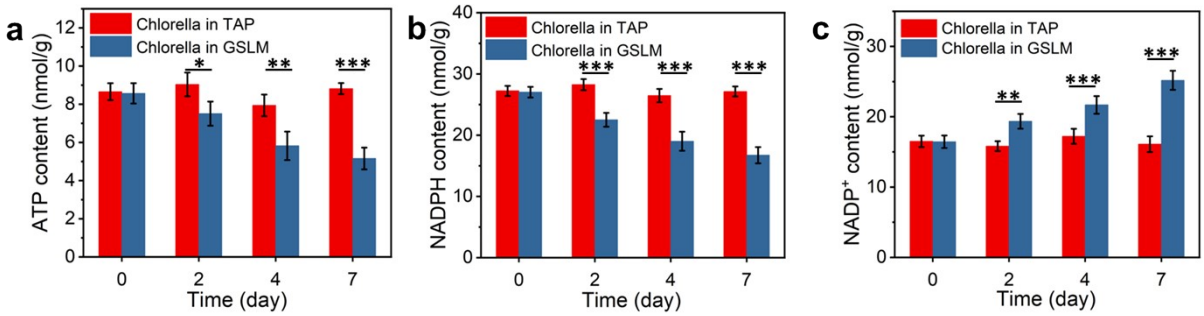

Figure S38. (a) ATP, (b) NADPH, and (c) $NADP^+$ contents of *Chlorella* in TAP and GSLM at 30 °C (n = 4, means ± SD). After *Chlorella* produced hydrogen in GSLM for 7 days, the contents of ATP and NADPH decreased by 39.8% and 38.1% as the content of $NADP^+$ (oxidized form of NADPH) increased by 53.1%.

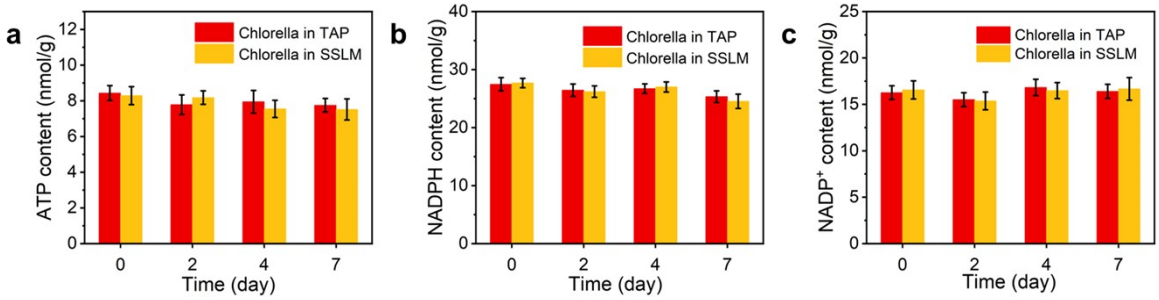

Figure S39. (a) ATP, (b) NADPH, and (c) $NADP^+$ contents of *Chlorella* in TAP and SSLM at 20 °C (n = 3, means ± SD). There was no significant difference in the contents of ATP, NADPH and $NADP^+$ of *Chlorella* in TAP and SSLM. PNIPAM-BA did not interfere with the metabolic processes related to ATP, NADPH and $NADP^+$ in *Chlorella*.

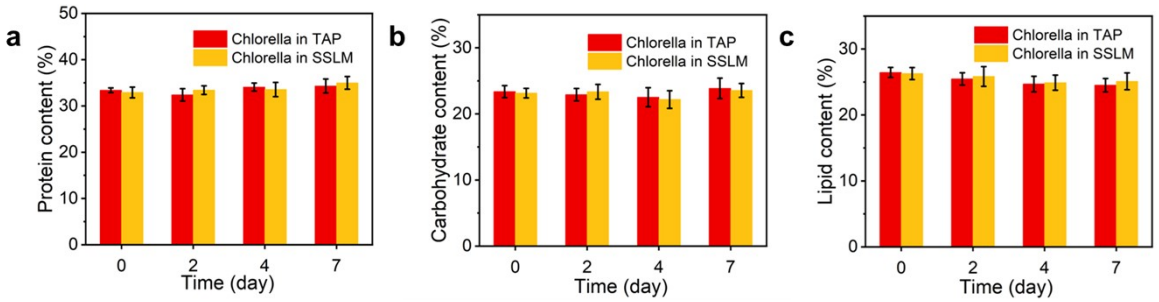

Figure S40. (a) protein, (b) carbohydrate, and (c) lipid contents of *Chlorella* were in TAP and SSLM at 20 °C, respectively (n = 3, means ± SD). We did not observe significant differences in protein, carbohydrate and lipid contents of *Chlorella* in SSLM or TAP media. PNIPAM-BA itself did not affect the protein, carbohydrate and lipid related metabolic processes of *Chlorella*.

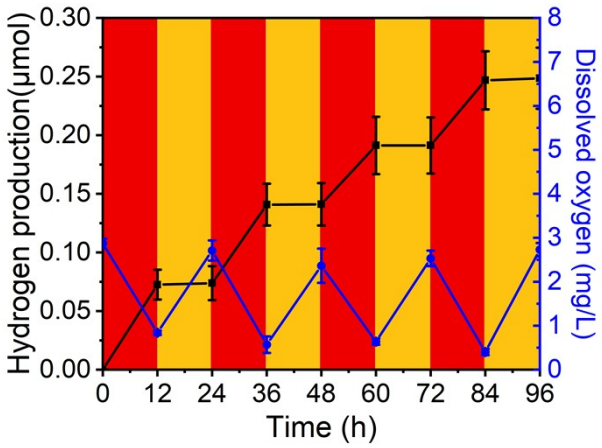

Figure S41. Tunable function of living material between H_2 production (black squares) and O_2 production (blue circles) through the transition of GSLM and SSLM. Red regions represented GSLM at 30 °C; Yellow regions represented SSLM at 20 °C (n = 4, means ± SD).

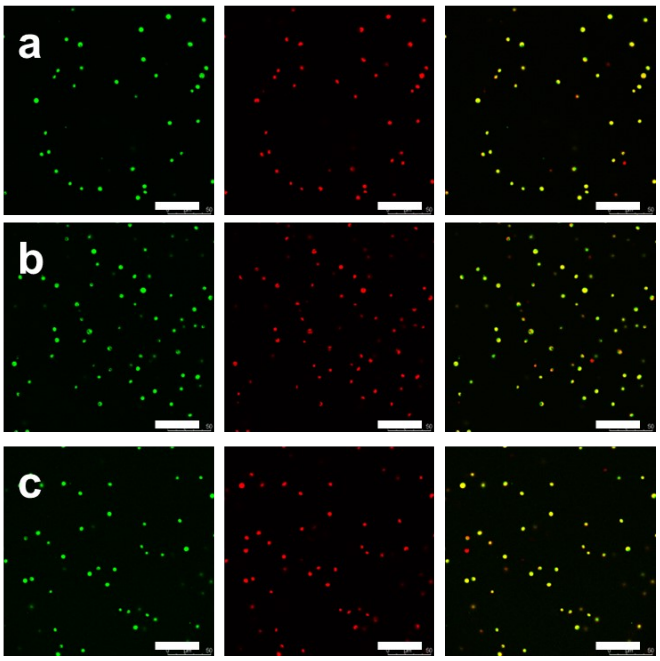

Figure S42. CLSM images for monitoring *Chlorella* activity in living material on day 15 (a), day 30 (b), day 45 (c) in TAP solution. The green fluorescence was from viable *Chlorella* and the red fluorescence was from intracellular chlorophyll. Scale bars, 50 μm.

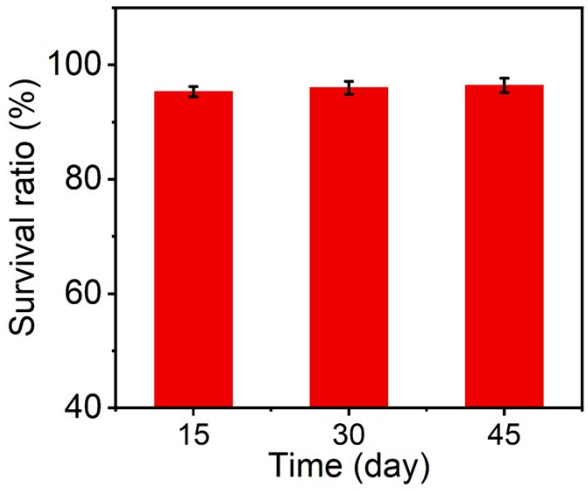

Figure S43. *Chlorella* survival ratio in living material on days 15, 30 and 45 (n = 3, means ± SD). *Chlorella* survival ratio was calculated by dividing the number of green fluorescent *Chlorella* by the number of red fluorescent *Chlorella*.

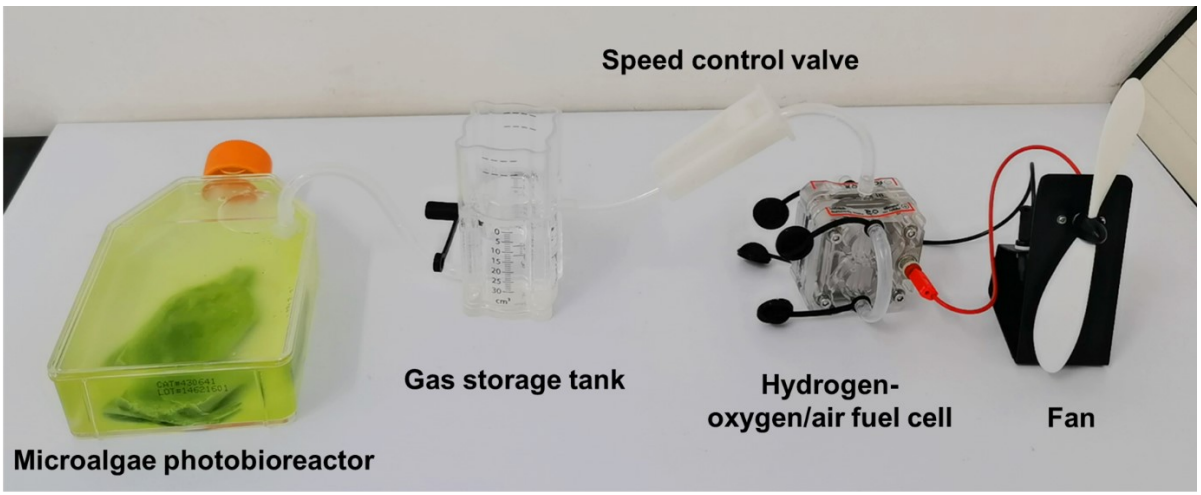

Figure S44. Demonstration of microalgae-generated hydrogen powering a fuel cell to drive a fan.

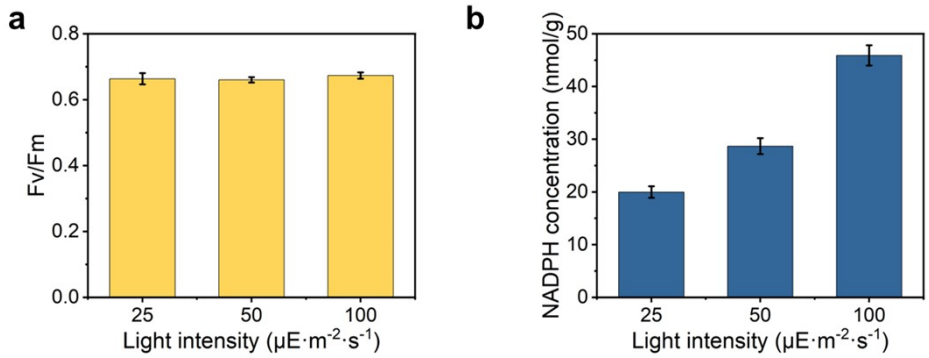

Figure S45. a Fv/Fm of natural *Chlorella* after incubation for 48 hours under different light intensities at 25 °C. **b** NADPH concentration of natural *Chlorella* after incubation for 48 hours under different light intensities at 25 °C.

The NADPH concentration of *Chlorella* was positively correlated with light intensity, but no significant difference was observed in Fv/Fm. The definition of Fv/Fm is maximal quantum yield of PS II, which does not vary with the light intensity received by the algae. Therefore, the shading effect of GSLM on core *Chlorella* did not change its Fv/Fm, which showed that the photosynthetic potential of the algae was well maintained. The light-dependent products (ATP and NADPH) were affected by the light intensity received by algae and had positive correlation. Therefore, the shading effect led to a decrease in the concentration of the light-dependent products.

Table S1. Changes in modulus, *Chlorella* concentration and volume shrinkage ratio in time-sweep experiments of living materials.

Time (min)	G' (Pa)	G" (Pa)	*Chlorella* concentration ($\times 10^7$cells/mL)	Volume shrinkage ratio
0	0.99	0.26	7.55	1.000
5	6.23×10^2	2.34×10^2	8.03	1.064
30	4.07×10^4	1.20×10^4	25.3	3.351
60	6.68×10^5	1.89×10^5	39.1	5.178
90	1.56×10^6	4.53×10^5	54.8	7.258
120	2.15×10^6	5.93×10^5	63.1	8.358
150	2.67×10^6	7.37×10^5	68.4	9.060

Table S2. Comparison of hydrogen production by microalgae.

Microalgae species	Light intensity ($\mu E \cdot m^{-2} \cdot s^{-1}$)	Average hydrogen production rate (based on chlorophyll concentration) ($\mu mol\ H_2$ (mg chlorophyll)$^{-1} h^{-1}$)	Average hydrogen production rate (based on light-receiving area) ($\mu mol\ H_2 \cdot m^{-2} \cdot h^{-1}$)	Culture medium	The longest hydrogen production time (day)	Anaerobic environment construction method	Average conversion efficiency of light energy to hydrogen energy (‰)	References
Chlorella pyrenoidosa	**50**	**0.11**	**61.43**	**TAP**	**45**	**Microalgae living material**	**0.378**	**1-This study**
Chlorella pyrenoidosa	100	0.32	74.36	TAP	15	Laccase catalyzed tannins	0.229	2-[13]
Chlamydomonas reinhardtii	80	0.44	128.21	TAP	26	Glucose oxidase oxidized glucose	0.493	3-[14]
Chlorella pyrenoidosa	100	0.25	50.27	TAP	7	High density microalgae spheroids	0.155	6-[15]
Chlamydomonas reinhardtii	120	0.19	52.32	TAP-S	9	Sulfur deprivation treatment	0.134	7-[16]
Chlamydomonas reinhardtii	120	0.63	173.58	TAP-S	17	Sulfur deprivation treatment + $Na_2S_2O_3$	0.445	8-[16]
Chlamydomonas reinhardtii	60	0.17	50.93	TAP-S	11	Sulfur deprivation treatment + Algal bacteria co-culture	0.261	9-[17]
Transgenic Chlamydomonas reinhardtii	60	0.35	102.37	TAP-S	19	Sulfur deprivation treatment + Algal bacteria co-culture	0.525	10-[17]

In view of the differences in light source intensity, photoreactor type and calculation method in each study, we attempted to normalize and quantitatively compare the hydrogen production capacity of microalgae using four parameters: hydrogen production rate based on chlorophyll concentration, hydrogen production rate based on light-receiving area, longest hydrogen production time and average light-to-hydrogen conversion

efficiency. Parameters for hydrogen production were re-calculated based on the information from the main text or supporting information only. The efficiency of light energy conversion to H_2 energy was calculated by the following equation[18]:

$$\eta\ (\%)=100\ \frac{(\Delta G^\circ - RT\ln((P^\circ/P))R_H}{EsA} = 100\ \frac{(\Delta G^\circ - RT\ln((P^\circ/P))Rs}{Es} \quad (10)$$

where ΔG° is the standard Gibbs free energy of H_2 (237200 J·mol^{-1} at 25 °C), R is the universal gas constant, T is the absolute temperature, P° and P are the standard and observed H_2 pressures (atm), R_H is the rate of H_2 photoproduction (μmol·h^{-1}), Rs is the rate of H_2 photoproduction per unit light-receiving area (μmol·m^{-2}·h^{-1}), E_S is the energy of the incident light radiation (averaged over 400 - 700 nm; 1 μE = 0.214 J, the energy of 1 mol of 560 nm photons), and A is the light-receiving area of the microalgae (m^2).

The average light-to-hydrogen conversion efficiency of microalgae achieved by our method of constructing living materials was on the same order as other studies in TAP or TAP-S. Then, we compared with studies (No. 9-10) with similar light source intensity, because the light source intensity affects the hydrogen production rate based on chlorophyll concentration, and found that it was similar to the system of No. 9. Based on the hydrogen production rate of the light-receiving area, the method we constructed had advantages over No. 6, No. 7 and No. 9. Moreover, our system used the respiration of microalgae to build an anaerobic environment without adding other chemicals, such as glucose (No. 3), tannic acid (No. 2), DMSO (No. 5) and sodium dithionite (No. 8), so it was relatively economical. In addition, our system had excellent hydrogen production capacity even at day 45, which was unmatched by other methods.

Video S1: Video about the preparation of living materials of different shapes.

Video S2: Video on the enrichment of PNIPAM-BA to the surface of microalgae during the sol-gel heating transition.

Video S3: Video of microalgae-generated hydrogen powering a fuel cell to drive a fan.

References

[1] M. Ehrbar, R. Schoenmakers, E.H. Christen, M. Fussenegger, W. Weber, Nat. Mater. 7 (2008) 800–804.

[2] H.Y. Yoshikawa, F.F. Rossetti, S. Kaufmann, T. Kaindl, J. Madsen, U. Engel, A.L. Lewis, S.P. Armes, M. Tanaka, J. Am. Chem. Soc. 133 (2011) 1367–1374.

[3] R.D. Harris, J.T. Auletta, S.A.M. Motlagh, M.J. Lawless, N.M. Perri, S. Saxena, L.M. Weiland, D.H. Waldeck, W.W. Clark, T.Y. Meyer, ACS Macro Lett. 2 (2013) 1095–1099.

[4] S. Zhang, D.J. Alvarez, M.V. Sofroniew, T.J. Deming, Biomacromolecules 16 (2015) 1331–1340.

[5] A.A. Abdeen, J. Lee, N.A. Bharadwaj, R.H. Ewoldt, K.A. Kilian, Adv. Healthc. Mater. 5 (2016) 2536–2544.

[6] M. Hörning, M. Nakahata, P. Linke, A. Yamamoto, M. Veschgini, S. Kaufmann, Y. Takashima, A. Harada, M. Tanaka, Sci Rep 7 (2017) 7660.

[7] M. Lufton, O. Bustan, B. Eylon, E. Shtifman-Segal, T. Croitoru-Sadger, A. Shagan, A. Shabtay-Orbach, E. Corem-Salkmon, J. Berman, A. Nyska, B. Mizrahi, Adv. Funct. Mater. 28 (2018) 1801581.

[8] J.V. Accardo, J.A. Kalow, Chem. Sci. 9 (2018) 5987–5993.

[9] M.R. Arkenberg, D.M. Moore, C.-C. Lin, Acta Biomater. 83 (2019) 83–95.

[10] M. Hörner, K. Raute, B. Hummel, J. Madl, G. Creusen, O.S. Thomas, E.H. Christen, N. Hotz, R.J. Gübeli, R. Engesser, B. Rebmann, J. Lauer, B. Rolauffs, J. Timmer, W.W.A. Schamel, J. Pruszak, W. Römer, M.D. Zurbriggen, C. Friedrich, A. Walther, S. Minguet, R. Sawarkar, W. Weber, Adv. Mater. 31 (2019) 1806727.

[11] Z. Cai, K. Huang, C. Bao, X. Wang, X. Sun, H. Xia, Q. Lin, Y. Yang, L. Zhu, Chem. Mater. 31 (2019) 4710–4719.

[12] P. Yuan, Y. Luo, Y. Luo, L. Ma, Biomater. Sci. 9 (2021) 2553–2561.

[13] D. Su, J. Qi, X. Liu, L. Wang, H. Zhang, H. Xie, X. Huang, Angew. Chem. Int. Ed. 58 (2019) 3992–3995.

[14] J. Chen, J. Li, Q. Li, S. Wang, L. Wang, H. Liu, C. Fan, Energy Environ. Sci. 13 (2020) 2064–2068.

[15] Z. Xu, S. Wang, C. Zhao, S. Li, X. Liu, L. Wang, M. Li, X. Huang, S. Mann, Nat. Commun. 11 (2020) 5985.

[16] J. He, L. Xi, X. Sun, B. Ge, D. Liu, Z. Han, X. Pu, F. Huang, Int. J. Hydrog. Energy 43 (2018) 15005–15013.

[17] S. Wu, X. Li, J. Yu, Q. Wang, Bioresour. Technol. 123 (2012) 184–188.

[18] S.N. Kosourov, M. Seibert, Biotechnol. Bioeng. 102 (2009) 50–58.